Combinatorial Regulation of *clpC* Expression During Sporulation in *Bacillus subtilis*

by

Khushi Panchal

A Paper Presented to the

Faculty of Mount Holyoke College in

Partial Fulfillment of the Requirements for

the Degree of Bachelors of Arts with Honor

Department of Biological Sciences

South Hadley, MA 01075

May 2025

This paper was prepared

under the direction of

Professor Amy Camp

for eight credits.

ACKNOWLEDGEMENTS

This thesis would not have been possible without the constant support, encouragement, and belief of my mentors, peers, friends, and family.

When I first came to Mount Holyoke from India, I had no idea how much this place would change me. Over the past four years, I've grown into someone more confident, curious, and unafraid to take up space—growth that has shaped both who I am and how I approach science and research. I still remember stepping into the Camp Lab as a nervous sophomore, quietly looking up to the seniors writing their theses, wondering if I'd ever get there. Now, as I write these final words, it feels surreal to have made it to this point.

I am endlessly grateful to my PI and mentor, Amy Camp, who took a chance on me when all I had was curiosity and a willingness to learn. You created a space for me to learn, make mistakes, and grow, and that is something I'll always carry with me. Some of my most formative moments came from our long conversations—troubleshooting, debating data, and refining questions. Thank you for challenging me, supporting me, and shaping the scientist I'm becoming.

To the Camp Lab members, past and present—you have been like a second family. Thank you for paving the way, for cheering me on, and for making the lab feel like home. A special shoutout to Team J2K2—Jen, Jade, Kim, and Chelsea. Doing this alongside you has been a privilege, and I wouldn't have wanted it any other way.

I'm also deeply grateful to Craig Woodard, Jared Schwartzer, Becky Packard, Becki Lijek, and all the professors who've guided me along the way. You pushed me to think deeper, be more critical and ask better questions. To Jenny Watermill—thank you for being more than just a supervisor at the CDC. Your mentorship, kindness, and confidence in me—especially during moments of self-doubt—have meant the world.

To my friends, who have endured my endless rants about failed experiments, writing struggles, and late nights in the lab—thank you. Tehani and Stella, you have been my rocks, and I truly couldn't have done this without you. Audrey, Lexie, Poojaa, Pranavi, Jetun, and Tana, your steady presence and encouragement, even from miles away, have helped and grounded me in so many ways.

Finally, to my family—Mumma, Papa, and Aashu—thank you for always listening, even when the science made no sense to you. Your unwavering support, fascination, and belief have been my greatest motivation. Mom and Dad, no words can truly express how much I appreciate the sacrifices you have made to give me the opportunities I have today. Every success I achieve is because of you. I love you.

Thank you all for being part of this journey.

TABLE OF CONTENTS

LIST OF FIGURES

LIST OF TABLES

ABSTRACT

Sporulation in the bacterium *Bacillus subtilis* is a tightly regulated developmental process triggered by stress or nutrient limitation. Sigma factors coordinate gene expression during this process by directing RNA polymerase to specific promoters. The *clpC* gene encodes an ATPase that partners with ClpP to degrade misfolded or unnecessary proteins, playing a crucial role in protein quality control and metabolic shutdown during sporulation. *clpC* is regulated by multiple sigma factor-dependent promoters and is expressed in the forespore, mother cell, and vegetative cells. Although essential for forming mature, heat-resistant spores, the contribution of each promoter to *clpC* expression and function remains unclear. To address this, I used CRISPR-Cas9 to generate deletion mutants targeting individual *clpC* promoters and a full upstream promoter knockout. A *clpC-gfp* reporter showed compartment-specific expression: one promoter drives forespore expression, another is active in the mother cell and vegetative cells, and a third has minimal activity. The full promoter knockout nearly eliminated *clpC* expression. Despite these differences, individual promoter deletions had no significant impact on sporulation efficiency, suggesting functional redundancy. The full promoter knockout generally sporulated normally but sometimes showed defects, indicating that very low *clpC* expression may suffice for sporulation or that compensatory mechanisms exist. Together, these findings highlight the complexity and flexibility of *clpC* regulation during sporulation.

CHAPTER 1: INTRODUCTION

Protein degradation is an essential and highly regulated process that occurs in all living cells, from prokaryotes to eukaryotes (Maupin-Furlow, 2011; Gottesman and Maurizi, 1992). It plays a critical role in maintaining cellular homeostasis by ensuring that proteins are synthesized, utilized, and degraded in a balanced and controlled manner. Proteins are fundamental to nearly every aspect of cell biology and function—they serve as transporters, structural components, immune defenders, and enzymes that drive biochemical reactions. In essence, proteins drive life at the molecular level by enabling metabolism, maintaining cellular structure, and regulating key processes such as water and ion balance in body fluids (LaPelusa and Kaushik, 2022).

However, proteins can become damaged or misfolded due to factors like cellular stress, mutations, or errors during translation. Accumulation of such aberrant proteins can be toxic, impairing cellular function and contributing to disease pathogenesis (LaPelusa and Kaushik, 2022). To prevent this, cells rely on degradation pathways to remove these damaged, misfolded, or excess proteins. This continuously ongoing process, known as general proteolysis, is essential for cellular quality control and overall health (Maupin-Furlow, 2011; Gottesman and Maurizi, 1992).

Beyond the removal of damaged proteins, degradation also plays a key regulatory role. By selectively degrading specific proteins at specific times and locations, cells can fine-tune critical processes. For example, during signal transduction, proteins often need to be degraded once they have fulfilled their role to avoid prolonged or inappropriate activity. This regulated proteolysis is triggered by specific signals and is crucial for the proper coordination of biological processes such as the cell cycle, gene expression, and stress responses (Maupin-Furlow, 2011; Gottesman and Maurizi, 1992).

1-1 Regulated Proteolysis in Bacteria

In bacteria, regulated proteolysis is central to many physiological functions, including stress adaptation, cell division, biofilm formation, pathogenesis, and developmental processes like sporulation (Konovalova et al., 2013; Dougan et al., 2002). By modulating the abundance and activity of regulatory proteins, proteolysis enables rapid adaptation to environmental changes and facilitates intercellular communication. This allows bacteria to modulate gene expression and coordinate developmental programs efficiently (Mahmoud and Chien, 2018; Konovalova et al., 2013; Molière and Turgay, 2013).

One key system that enables this regulation involves the AAA+ (ATPases Associated with diverse cellular Activities) family of proteins. These ATP-dependent enzymes function as part of large protease complexes that typically include two components: an ATP-dependent unfoldase and a proteolytic peptidase. The unfoldase recognizes and processes target proteins, while the peptidase breaks them down into smaller peptides (Mahmoud and Chien, 2018; Konovalova et al., 2013).

In bacterial cells, major AAA+ proteases include Clp, HslUV, FtsH, and Lon. Notably, FtsH and Lon are single-chain proteases, wherein both the ATPase and peptidase domains are encoded within the same polypeptide chain. In contrast, Clp and HslUV are multi-subunit systems in which the ATPase and the peptidase exist as separate proteins that assemble into a functional complex (Mahmoud and Chien, 2018; Konovalova et al., 2013).

Among these, the Clp (caseinolytic protease) family is particularly versatile, with various possible combinations of unfoldase and peptidase subunits. Hexameric ATPases such as ClpC, ClpE, and ClpX identify target substrates by recognizing specific degradation signals (degrons) and use ATP hydrolysis to unfold them. These unfolded proteins are then translocated into the

ClpP proteolytic core, a barrel-shaped structure made of two stacked heptameric rings. The proteolytic active sites are sequestered inside the chamber, ensuring that degradation only occurs once substrates are fully translocated. This modular arrangement allows Clp complexes to handle a wide variety of substrates with high specificity and efficiency (Molière and Turgay, 2013; Kirstein et al., 2008; Sauer et al., 2004).

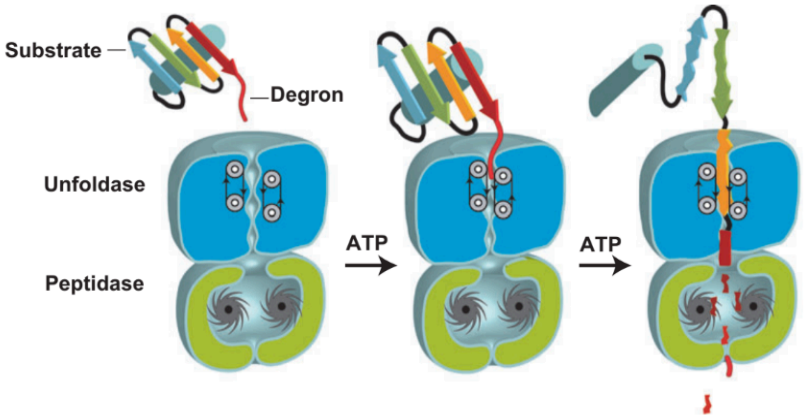

Figure 1. Schematic diagram of the AAA+ protease complex machinery. The ATPase (unfoldase) component utilizes energy from ATP hydrolysis to unfold substrate proteins and translocate them into the proteolytic chamber formed by the peptidase component, where degradation into peptides occurs (from Sauer and Baker, 2011).

These AAA+ protease complexes are widely conserved across bacterial species and represent promising targets for novel antimicrobial therapies, especially as more and more bacteria become antibiotic resistant (Aljghami et al., 2022; Maurer et al., 2019; Culp and Wright, 2017). For instance, acyldepsipeptide (ADEP) antibiotics bind to ClpP, deregulating its proteolytic activity and leading to uncontrolled degradation of essential proteins, including the cell division protein FtsZ, ultimately causing bacterial cell death. This mechanism has shown efficacy against persistent infections and multidrug-resistant pathogens (Reinhardt et al., 2022; Culp and Wright, 2017). Similarly, armeniaspirol, a natural product, inhibits the AAA+ proteases

ClpXP and ClpYQ, disrupting bacterial cell division and demonstrating potent antibacterial activity (Labana et al., 2021).

1-1-1 The ClpCP Complex

A prominent example of an AAA+ protease in Gram-positive bacteria is the ClpCP complex, which plays a crucial role in various cellular processes. This includes maintaining protein homeostasis and responding to stress conditions like heat shock, oxidative stress, and nutrient deprivation (Aljghami et al., 2022; Gerth et al., 2004).

In *Bacillus subtilis*, ClpCP regulates sporulation by degrading key regulatory proteins, ensuring proper developmental progression (Massoni et al., 2025; Pan and Losick, 2003; Krüger et al., 1994). Additionally, it is involved in the development of genetic competence, a state that enables cells to take up extracellular DNA (Turgay et al. 1998). In *Staphylococcus aureus*, ClpCP modulates energy metabolism, particularly influencing aerobic respiratory growth, and is implicated in controlling virulence factors such as capsule formation (Aljghami et al., 2022; Mashruwala et al. 2019). Similarly, in *Listeria monocytogenes*, ClpCP contributes to stress response and virulence functions, highlighting its role in pathogenesis (Aljghami et al., 2022; Nair et al., 2000). In *Mycobacterium tuberculosis*, ClpC is a direct target for several antibiotics, including Cyclomarin A, lassomycin, rufomycin, and ecumicin (Choules et al., 2019; Maurer et al., 2019; Gao et al., 2015; Gavrish et al., 2014).

The widespread presence and multifaceted functions of the ClpCP complex underscore its evolutionary significance and potential as a target for microbial therapeutics, making it a subject of interest for many researchers.

1-1-2 Adaptor Proteins in ClpC-Mediated Proteolysis

Adaptor proteins are crucial modulators of AAA+ protease complexes, enhancing substrate binding specificity and chaperone activity (Dougan et al., 2002). These adaptors, typically small and structurally diverse, modulate AAA+ protein activity either by binding directly to substrates or by altering substrate recognition once the complex forms (Kirstein et al., 2009; Dougan et al., 2002).

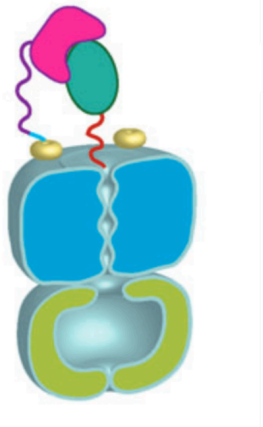

Figure 2. Schematic representation of the AAA+ protease complex with associated adaptor proteins. Adaptor proteins bind to the AAA+ unfoldase component, modulating substrate specificity and facilitating the recognition and delivery of targeted proteins to the proteolytic chamber for degradation (from Sauer and Baker, 2011).

While many AAA+ proteases can function independently, studies suggest that ClpC remains inactive until it binds to specific adaptors, which induce its oligomerization into an active hexameric form (Kirstein et al., 2008; Kirstein et al., 2006; Schlothauer et al., 2003). Several adaptors have been identified for ClpC across different bacteria, each conferring distinct functional specificities (Dougan et al., 2002; Kirstein et al., 2009).

In *B. subtilis*, one of the best-studied and characterized adaptors is MecA, which regulates the stability of ComK, a master regulator of genetic competence. MecA binds to ComK and ClpC, forming a ternary complex that targets ComK for degradation via the ClpCP protease.

This mechanism prevents premature competence development under non-inducing conditions. During competence—triggered by quorum-sensing signals—MecA is sequestered or inactivated, allowing ComK to accumulate and activate genes required for DNA uptake and transformation (Konovalova et al., 2013; Dougan et al., 2002; Turgay et al., 1998).

Other established adaptors in *B. subtilis* include YpbH and McsB (Dougan et al., 2002; Kirstein et al., 2007; Kirstein et al., 2009). Recently, a novel ClpC adaptor protein, MdfA (metabolic differentiation factor A; formerly YjbA), has been identified. MdfA is specifically expressed in the forespore during sporulation and associates with ClpC to degrade metabolic enzymes and transcription factors, enabling the metabolic shutdown necessary for spore formation (Massoni et al., 2025; Riley et al., 2025).

1-2 *Bacillus subtilis*: A Model System

B. subtilis is a gram-positive, rod-shaped bacterium found abundantly in soil and in the gastrointestinal tracts of various animals (Earl et al., 2008). It is one of the most extensively studied prokaryotes due to its genetic tractability, rapid growth, and well-defined regulatory pathways (Harwood, 2007; Su et al., 2020). The laboratory strain *B. subtilis* 168, a tryptophan auxotroph isolated in the 1950s, was among the first bacterial genomes to be sequenced, revealing a 4.2 Mbp chromosome encoding approximately 4,100 genes (Kunst et al., 1997). This comprehensive genomic information has further facilitated in-depth studies into its physiology and genetics (Zeigler et al., 2008).

Classified as Generally Recognized As Safe (GRAS) by the U.S. Food and Drug Administration (FDA), *B. subtilis* is non-pathogenic and widely used in both academic and industrial settings. Its evolutionary relatedness to pathogenic species like *Bacillus anthracis* and commonalities with other spore forming bacteria like *Clostridium spp.* also makes it a valuable

model for studying bacterial pathogenesis and stress resistance (Zhu et al., 2018; Singh et al., 2014). Its natural competence—the ability to uptake exogenous DNA from the environment—facilitates straightforward genetic manipulation (Harwood, 2007). Moreover, its adaptive features, including biofilm formation and sporulation, allow it to survive environmental stress, further supporting its use as a model organism (Tan and Ramamurthi, 2014).

1-2-1 Sporulation in *B. subtilis*

In response to stressful environmental conditions like nutrient limitation, high temperature, or desiccation, *B. subtilis* initiates sporulation—a highly coordinated, multi-stage developmental process that produces a dormant and highly resistant endospore. These spores are metabolically inactive, partially dehydrated structures that can persist in harsh environments for extended periods (Tan and Ramamurthi, 2014).

Sporulation begins with asymmetric division of a vegetative cell upon sensing stress conditions. Instead of dividing symmetrically to produce two identical daughter cells, the bacterium divides near one pole, producing a smaller compartment known as the forespore and a larger compartment called the mother cell (Tan and Ramamurthi, 2014). This division occurs through the formation of a polar septum and leads to the unequal distribution of the chromosome: about one-third enters the forespore while the remaining two-thirds stays in the mother cell (Frandsen et al., 1999). This genetic asymmetry is temporary, as the rest of the chromosome is later pumped into the forespore, but it is essential in establishing the identity and developmental trajectory of each compartment (Frandsen et al., 1999).

The asymmetric division initiates a cascade of gene expression changes driven by compartment-specific sigma factors (Bradshaw and Losick, 2015; Frandsen et al., 1999). These sigma factors are transcriptional regulators that activate distinct sets of genes required for each

stage of sporulation, ensuring that molecular events occur at the right time and place in the developing spore.

Following septation, the mother cell engulfs the forespore through a phagocytosis-like process, enclosing the forespore within the mother cell's cytoplasm (Tan and Ramamurthi, 2014). This results in a double-membrane-bound forespore, isolating it from the external environment and limiting its metabolic activity (Camp and Losick, 2009). The Camp Lab has previously identified a "feeding tube" model, where proteins SpoIIIAA and SpoIIIAH in the mother cell, produced under σ^E control, and forespore protein SpoIIQ, produced under σ^F control, interact to form a gap-junction-like channel. This channel allows the mother cell to transport small molecules, such as ATP and metabolites, to the forespore, supporting its development and the expression of genes required for the progression of sporulation (Camp and Losick, 2009; Meisner et al., 2008).

Once engulfed, the forespore undergoes the formation of a thick peptidoglycan cortex between its two membranes. This cortex is essential for maintaining spore dehydration and dormancy (Setlow, 2006). Concurrently, the mother cell synthesizes a multilayered protein coat around the forespore, comprising over 70 distinct proteins organized into four layers: the basement layer, inner coat, outer coat, and crust (Tan and Ramamurthi, 2014). These layers enhance the spore's resistance to chemical and enzymatic degradation. Within the spore core, DNA becomes densely packed and associates with small acid-soluble spore proteins (SASPs), which alter DNA structure and provide protection against UV radiation and heat. Additionally, the accumulation of dipicolinic acid (DPA) and calcium ions further contribute to the spore's heat resistance and stability (Setlow, 2006).

Once spore maturation is complete, the mother cell undergoes programmed cell death and lyses, releasing the mature endospore into the environment. The dormant spore remains inactive until it encounters favorable conditions—such as the presence of nutrients and optimal temperatures—at which point it can germinate and re-enter the vegetative growth cycle (Tan and Ramamurthi, 2014). Throughout sporulation, sigma factor mediated regulation of gene expression and selective protein degradation ensure precise control of each developmental stage.

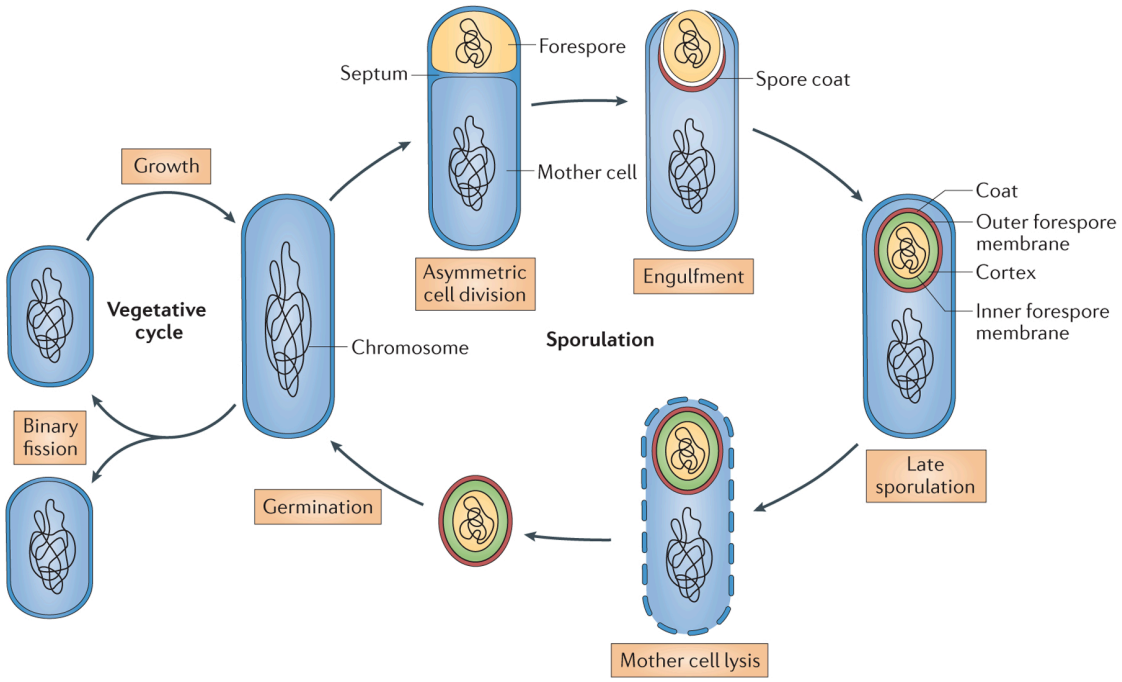

Figure 3. Stages of Sporulation in *B. subtilis*. Under normal conditions, *B. subtilis* divides by binary fission. However, under stress, it initiates a distinct developmental pathway, starting with asymmetric cell division that forms a forespore and a mother cell. The forespore is engulfed by the mother cell and surrounded by a protective peptidoglycan cortex and a multilayered protein coat, which is synthesized by the mother cell. This process results in the formation of a highly resilient spore, capable of surviving for prolonged periods until favorable conditions return and the cell resumes normal vegetative growth (from McKenney et al., 2012).

1-3 Gene Expression Regulation by Sigma Factors

In *B. subtilis*, gene expression is primarily regulated at the transcriptional level by sigma factors (Haldenwang, 1995; Wösten, 1998). These proteins are essential for the initiation of transcription, as they recognize and recruit RNA polymerase (RNAP) to specific promoter sequences, thereby facilitating the transcription of target genes. Sigma factors associate transiently with the RNAP core, which consists of α, α, β, and β' subunits, to form the RNAP holoenzyme—the functional complex responsible for transcription initiation (Wösten, 1998).

Each sigma factor recognizes conserved promoter sequences located at the -35 and -10 regions upstream of the transcription start site (Wösten, 1998). The distinct consensus sequence of each sigma factor dictates its binding specificity, allowing different sigma factors to regulate unique sets of genes. This specificity ensures precise control over transcription, enabling *B. subtilis* to coordinate gene expression in response to changing environmental conditions and developmental needs (Haldenwang, 1995).

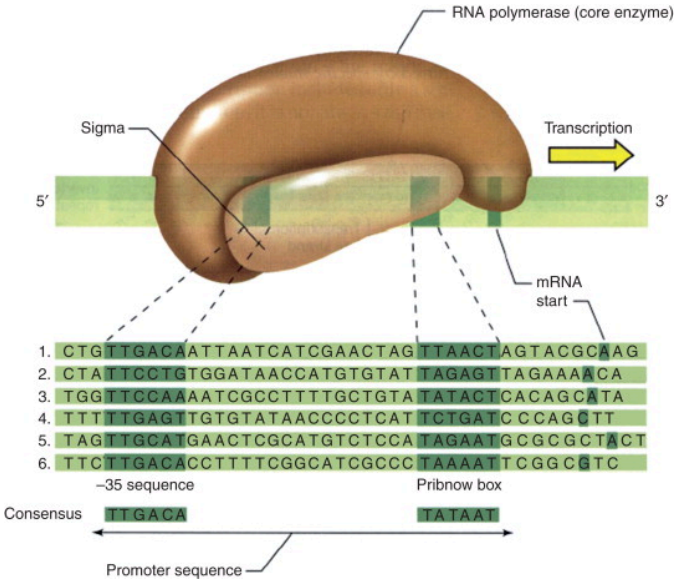

Figure 4. Schematic representation of sigma factor and RNA polymerase core at the promoter site. The sigma factor directs the RNA polymerase core enzyme to the -10 and -35 promoter elements, facilitating specific binding and transcription initiation of downstream genes (from *Encyclopedia of Microbiology*, 3rd Edition, 2009).

The primary housekeeping sigma factor in *B. subtilis* is σ^A, and it directs the transcription of genes required for routine cellular functions and vegetative growth (Haldenwang, 1995). In addition to σ^A, *B. subtilis* employs a variety of alternative sigma factors that regulate gene expression in response to specific stimuli or developmental transitions (Haldenwang, 1995). For example, σ^B is activated under stress conditions and coordinates the general stress response, enabling the bacterium to survive unfavorable conditions such as heat shock, osmotic stress, or energy depletion (Rodriguez Ayala et al., 2020; Wösten, 1998). In contrast, σ^H plays a crucial role in the transition from exponential to stationary phase and is also involved in the early stages of sporulation and competence development (Haldenwang, 1995; Wösten, 1998).

A specialized set of alternative sigma factors called the sporulation-specific sigma factors govern sporulation in a compartmentalized and sequential manner, directing gene expression in either the forespore or the mother cell (Fimlaid and Shen, 2015).

Sigma factor (alternative designation)	Gene(s)	Function	Promoter sequence[b]		
			−35	Spacer (bp)	−10
Vegetative-cell factors					
σ^A (σ^{43}, σ^{55})	*sigA*, *rpoD*	Housekeeping/early sporulation	TTGACA	17	TATAAT
σ^B (σ^{37})	*sigB*	General stress response	RGGXTTRA	14	GGGTAT
σ^C (σ^{32})	Unknown	Postexponential gene expression	AAATC	15	TAXTGYTTZTA
σ^D (σ^{28})	*sigD*, *flaB*	Chemotaxis/autolysin/flagellar gene expression	TAAA	15	GCCGATAT
σ^H (σ^{30})	*sigH*, *spoOH*	Postexponential gene expression; competence and early sporulation genes	RWAGGAXXT	14	HGAAT
σ^L	*sigL*	Degradative enzyme gene expression	TGGCAC	5	TTGCANNN
Sporulation-specific factors					
σ^E (σ^{29})	*sigE*, *spoIIGB*	Early mother cell gene expression	ZHATAXX	14	CATACAHT
σ^F ($\sigma^{spoIIAC}$)	*sigF*, *spoIIAC*	Early forespore gene expression	GCATR	15	GGHRARHTX
σ^G	*sigG*, *spoIIIG*	Late forespore gene expression	GHATR	18	CATXHTA
σ^K (σ^{27})	*sigK*, *spoIVCB*:*spoIIIC*	Late mother cell gene expression	AC	17	CATANNNTA

Figure 5. Sigma factors in *B. subtilis.* Overview of sigma factors in *B. subtilis*, detailing their associated structural genes, primary functions, and preferred promoter recognition sequences. The consensus sequences for the −35 and −10 promoter regions are aligned at their respective positions, with the spacer region indicating the number of nucleotides between these elements. (from Haldenwang, 1995).

1-3-1 Sporulation-Specific Sigma Factors

Sporulation-specific sigma factors—σ^F and σ^G in the forespore, and σ^E and σ^K in the mother cell—are activated at distinct stages and regulate key genes necessary for morphological and biochemical changes during spore development (Tan and Ramamurthi, 2014).

σ^F is the first to be activated following asymmetric division and is restricted to the forespore. Its activation is tightly regulated by a phosphorelay system. Initially, σ^F is held inactive by the anti-sigma factor SpoIIAB. SpoIIE, a septum-localized phosphatase, dephosphorylates SpoIIAA in the forespore, which then binds to SpoIIAB and frees σ^F to initiate transcription. σ^F directs early forespore gene expression, including the transcription of *spoIIR*, a key signal that activates σ^E in the mother cell and promotes coordinated progression of sporulation (Carniol et al. 2004; Piggot and Hilbert, 2004; Pan and Losick, 2003).

Subsequently, σ^E becomes active in the mother cell and regulates genes involved in membrane remodeling and engulfment. After the forespore is engulfed, σ^G is activated in the forespore and governs late-stage forespore gene expression, including DNA protection and spore coat formation. Activation of σ^G also leads to the signaling events that trigger σ^K activation in the mother cell. σ^K regulates the final stages of sporulation, including spore maturation and assembly of outer layers (Tan and Ramamurthi, 2014; Piggot and Hilbert, 2004).

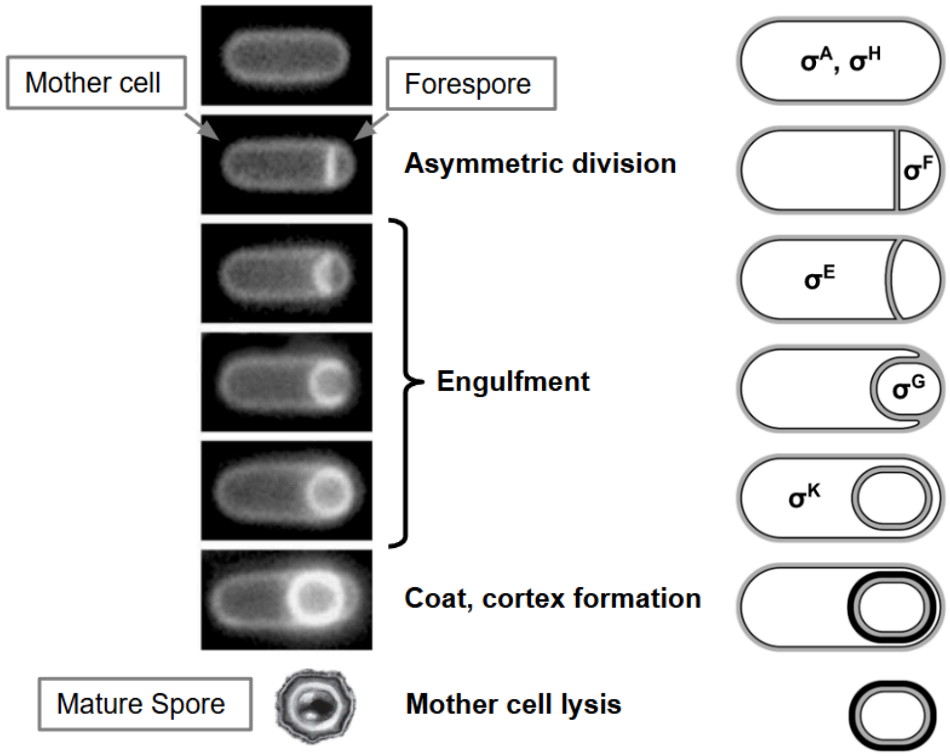

Figure 6. Spatial and temporal activation of sigma factors during sporulation. The left panel shows the morphological stages of sporulation, while the right schematic outlines the sequential activation of sigma factors in different compartments. σ^F is activated in the forespore after asymmetric division, followed by σ^E in the mother cell. σ^G is activated in the forespore post-engulfment, and σ^K becomes active in the mother cell during late sporulation.

1-4 Role of ClpCP in Sporulation

Sporulation involves extensive cellular remodeling and metabolic reprogramming, processes that rely heavily on regulated protein degradation. The ClpCP protease complex, along with the adaptor MdfA, plays a key role in orchestrating these changes (Massoni et al., 2025; Riley et al., 2025; Pan et al. 2001).

One of ClpCP's key functions is controlling the timing of sporulation initiation. It targets the unphosphorylated, inactive form of Spo0A—the master regulator of sporulation—for degradation, thereby preventing premature entry into the sporulation pathway. Additionally, ClpCP degrades SpoIIAB, an anti-sigma factor that inhibits σ^F. The degradation of SpoIIAB

releases σ^F, the forespore-specific sigma factor critical for early sporulation gene expression (Kain et al., 2008; Meeske et al., 2016; Pan et al., 2001).

Recent studies have shown that ClpCP, aided by the adaptor protein MdfA, degrades forespore metabolic enzymes and transcription factors following polar septation. This activity supports the metabolic shutdown of the forespore and increases its reliance on the mother cell (Massoni et al., 2025; Riley et al., 2025).

Targeted proteolysis by ClpCP is hence essential for stage-specific gene expression and the formation of viable spores. Studies have shown that mutant strains lacking either *clpC* or *clpP* exhibit severe sporulation defects, with spore production reduced by 3–4 orders of magnitude compared to wild-type, underscoring ClpCP's importance to the process (Meeske et al. 2016; Singh et al., 2014; Pan and Losick, 2003).

Interestingly, Δ*mdfA* mutants sporulate at wild-type levels, suggesting that while MdfA is required for the degradation of certain substrates, ClpCP also operates through MdfA-independent pathways (unpublished Camp Lab data). As such, further investigation into the transcriptional regulation of *clpC* is necessary to understand its broader role in the sporulation process.

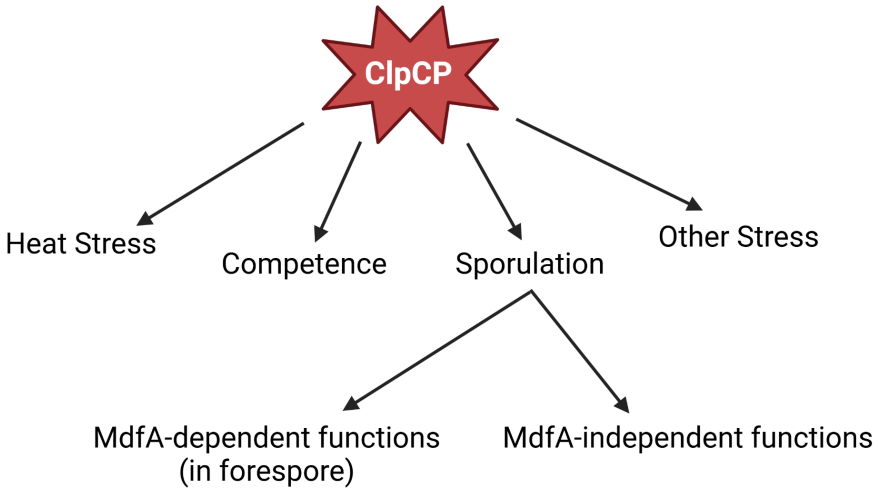

Figure 7. The diverse functional roles of ClpCP. The ClpCP protease complex is involved in multiple cellular processes, including heat stress response, competence, and sporulation. During sporulation, ClpCP regulates two distinct pathways: an MdfA-dependent and an MdfA-independent pathway (made using BioRender).

1-5 Regulation of the *clpC* Operon

The *clpC* operon in *B. subtilis* comprises four genes: *ctsR, mcsA, mcsB,* and *clpC*, each contributing to the cell's stress response mechanisms (Krüger and Hecker, 1998).

ctsR, the first gene in the operon, encodes a transcriptional repressor that inhibits the expression of *clpC, clpP* and other class III heat shock genes under non-stress conditions. It achieves this by binding to a conserved heptanucleotide direct repeat sequence located upstream of target genes, thereby repressing their transcription (Krüger and Hecker, 1998; Derré et al., 1999). This binding site is also present upstream the *clpC* operon, and facilitates an autoregulatory feedback loop, maintaining appropriate expression levels of the operon's genes. Upon stress induction, modifications to CtsR, influenced by McsA and McsB, result in derepression of the operon and enhanced expression of stress response proteins essential for bacterial survival (Krüger and Hecker, 1998).

Adjacent to *ctsR* are *mcsA* and *mcsB*, which encode proteins that modulate CtsR activity. McsB is a protein arginine kinase that phosphorylates CtsR, reducing its DNA-binding affinity and alleviating repression (Fuhrmann et al., 2009; Kirstein et al., 2005). McsA acts as an activator of McsB, enhancing its kinase activity (Kirstein et al., 2005). The interplay among McsA, McsB, and CtsR ensures a finely tuned response to environmental stressors.

The final gene, *clpC*, encodes the ATP-dependent unfoldase ClpC that collaborates with the peptidase ClpP to form the ClpCP protease complex (Krüger et al., 1996). ClpC is present in both vegetative and sporulating cells, suggesting that it plays complex and varied roles in a cell's life cycle, depending on the environmental conditions and cues that it is exposed to (Rodriguez Ayala et al., 2020; Schlothauer et al., 2003; Pan et al., 2001; Krüger et al., 2000). This versatility is facilitated mainly due its combinatorial regulation by different sigma factors activated under specific conditions, allowing the cell to produce ClpC in a highly regulated manner (Krüger et al., 1996).

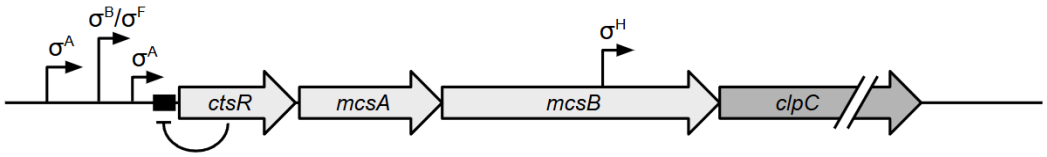

Figure 8. *clpC* Operon and Its Sigma Factor-Dependent Regulatory Regions. The *clpC* operon consists of four genes: *ctsR*, *mcsA*, *mcsB*, and *clpC*, with a CtsR binding site (black box) upstream of the *ctsR* gene. Under normal conditions, CtsR binds to this site, repressing the transcription of the operon. However, under stress conditions, this repression is relieved, initiating transcription of the operon. The operon is regulated by four sigma factor-dependent promoters: three located upstream of the operon recognized by σ^A, σ^B/σ^F, and σ^A, and one within the *mcsB* gene recognized by σ^H.

1-5-1 Sigma-factor dependent promoters regulating the *clpC* operon

Bioinformatic analyses have identified several sigma factor-dependent promoters regulating the *clpC* operon, based on conserved consensus sequences. While some predicted

promoters were experimentally validated, others were shown to be inactive and excluded from further investigation. According to current understanding, there are four sigma factor-dependent promoter sites that regulate the *clpC* operon (Berg, 2023; Quigley, 2023; Mayangsari, 2018; Nkomboni, 2017).

Three of these promoters are located upstream of the operon, while a fourth, σ^H-dependent promoter, lies within the *mcsB* gene. Previous experiments by a former student demonstrated that Δ*mcsB* mutants lacking the σ^H-dependent promoter sporulate at wild-type levels, suggesting this promoter is not essential for sporulation (Quigley, 2023). Consequently, my work focused on the remaining three promoters located upstream of the operon.

Among these upstream promoters, the vegetative σ^A promoter directly upstream of *ctsR* is the most extensively studied, along with the general stress response σ^B promoter. Both have been shown to be active and contributing to *clpC* expression under different conditions (Krüger and Hecker, 1998; Krüger et al., 1996). In addition, further work in our lab has led to the identification of a putative σ^F consensus sequence overlapping with the σ^B site. While unpublished, there is strong evidence suggesting that this region may be co-regulated by both sigma factors (unpublished Camp Lab data; He, 2010). Lastly, there was a transcriptomic study conducted by Nicolas et al. (2012) that suggested the presence and activity of an additional promoter σ^A promoter further upstream. However, beyond the transcriptomic mention, there is little published literature regarding this promoter, and it had not been characterized in our lab prior to this study.

A prior study by Kain et al. (2008) showed that *clpC* expression increases in the forespore during early sporulation. They proposed that this boost is driven by σ^F activation,

which is triggered by ClpCP-mediated degradation of SpoIIAB. Once active, σ^F promotes additional *clpC* expression, forming a positive feedback loop that reinforces ClpCP function.

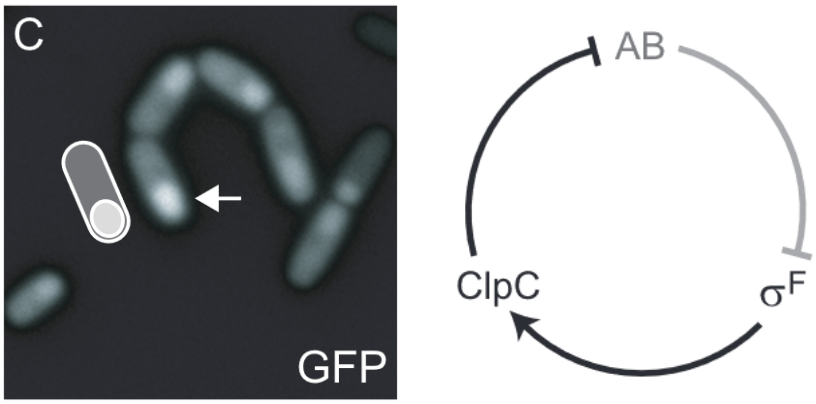

Figure 9. Elevated *clpC* expression in the forespore. (a) Microscopy image showing boost in *clpC* expression in the forespore. (b) Schematic of the feedback loop in which ClpC-mediated degradation of SpoIIAB relieves repression of σ^F, leading to further upregulation of *clpC* (from Kain et al., 2008).

Initially, we hypothesized that this σ^F-mediated expression boost was essential for ClpC function and sporulation. However, parallel experiments by a colleague—who generated a σ^B/σ^F promoter deletion mutant and introduced point mutations disrupting σ^F recognition—revealed that these mutants sporulated without any defects. This suggested that while σ^F may contribute to *clpC* expression, it is not required for forming heat-resistant spores (unpublished Camp Lab data).

These findings, along with growing evidence for ClpCP's diverse functions, led us to investigate how the upstream promoters contribute to *clpC* regulation. To do this, I generated deletion mutants of the two σ^A-dependent promoters and a full upstream promoter region knockout. Additionally, I characterized the σ^B/σ^F-dependent promoter created by a different lab member. By analyzing *clpC* expression in these strains using a *clpC-gfp* reporter system and assessing their sporulation efficiency, this study aims to clarify how each promoter contributes to the transcriptional regulation and function of ClpC during sporulation.

CHAPTER 2: MATERIALS AND METHODS

2-1 General Methods

Bacterial strains were streaked and plated on Luria-Bertani (LB) agar plates and incubated at 37˚C to grow overnight. Selective media containing the appropriate antibiotics were used as needed, depending on the experiment. Liquid cultures were grown in LB media or other specified media in a roller drum incubator at 37°C. Strains were stored as glycerol stocks by mixing 900 µL of overnight culture with 600 µl of sterile 50% glycerol in cryo tubes. All glycerol stocks were stored at –80°C.

2-2 DNA Amplification and Purification

Polymerase chain reactions (PCR) were performed using either Phusion High-Fidelity DNA Polymerase or Taq DNA Polymerase (New England Biolabs (NEB)). Taq polymerase was used for amplification from chromosomal DNA, while Phusion was used for cloning and mutagenesis. Annealing temperatures were adjusted based on primer length and GC content. Some reactions required further optimization with HF Buffer and DMSO.

Agarose gel electrophoresis was performed using 1% agarose gels in 1× TAE buffer with GelRed stain. Gels were run at 120V for 30–40 minutes and visualized under UV light. PCR-amplified DNA was purified using the Monarch® PCR & DNA Cleanup Kit (NEB) following the manufacturer's protocol.

2-3 Plasmid Construction: pKP1 Assembly

The CRISPR plasmid pKP1 was constructed by inserting a *ctsR* repair template into the pAJS23 backbone (Sachla et al., 2021). The PCR-based FastCloning technique (Li et al., 2011) was used for assembly. Primers oKP1/oKP2 were designed to amplify the *ctsR* repair template

with overhangs complementary to pAJS23, and primers oSY1/oSY2 were used to linearize the pAJS23 plasmid. All primer sequences were designed using the NEBuilder Assembly Tool.

PCR products were confirmed via gel electrophoresis and purified. DpnI digestion was performed at 37°C for 2 hours to remove methylated parental plasmid DNA. A 1:2 mixture of linearized pAJS23 (5 μL) and repair template (10 μL) was used for transformation into *Escherichia coli*.

2-3-1 Transformation into *E. coli*

NEB 10-beta competent *E. coli* cells were thawed on ice and transformed with 2 μL of DNA. Cells were incubated on ice for 30 minutes, heat-shocked at 42°C for 30 seconds, then placed back on ice for 5 minutes. Recovery was performed in 950 μL of NEB 10-beta/Stable Outgrowth Medium at 37°C with shaking for 1 hour. After recovery, 100 μL was plated on LB agar plates supplemented with 30 μg/mL kanamycin (LB/Kan30). The remainder was pelleted, resuspended in ~200 μL, and plated to maximize colony yield. Plates were incubated overnight at 37°C. The appearance of colonies on the transformation plates indicated successful uptake of the plasmid containing the kanamycin resistance gene.

2-3-2 Plasmid Isolation and Verification

Plasmid DNA was isolated from random individual colonies using the NucleoSpin® Plasmid Mini kit (Macherey-Nagel). Plasmids were digested with XmnI to confirm insertion of the repair template and analyzed via gel electrophoresis. Plasmids with correct banding patterns were submitted for Nanopore sequencing. A confirmed plasmid containing the intact *ctsR* repair template without unintended mutations was designated pKP1.

2-4 Site-Directed Mutagenesis: pKP3, pKP4, pKP5 Construction

Three promoter deletion constructs were generated from pKP1 using site-directed mutagenesis following the protocol by Liu and Naismith (2008). Deletion constructs included: (1) ΔPA1 (oKP3/oKP4), (2) ΔPA2 (oKP5/oKP6), and (3) ΔPFull (oKP7/oKP8). Primers were designed with complementary overhangs flanking the targeted deletion sites.

Each mutagenesis reaction was amplified and verified on agarose gels, and subsequently, purified and treated with DpnI to eliminate parental plasmid DNA. Mutagenized DNA was transformed into NEB 10-beta *E. coli* using the previously described protocol and selected on LB/Kan30.

Colonies were mini-prepped using the NucleoSpin® Plasmid (NoLid) kit and quantified using a NanoDrop spectrophotometer. All constructs were validated by Nanopore sequencing to confirm successful deletions and the absence of off-target mutations.

Table 1. Plasmids used in this study

Name	Genotype	Construction/Source
pKP1	pAJS23 backbone + *ctsR* repair template	Constructed by integrating *ctsR* repair template into pAJS23 using FastCloning (Li et al., 2011)
pKP3	ΔPA1 → pKP1	pKP1 with deletion of the downstream σ^A promoter (PA1) created using primers oKP3/oKP4
pKP4	ΔPA2 → pKP1	pKP1 with deletion of the upstream σ^A promoter (PA2) created using primers oKP5/oKP6
pKP5	ΔPFull → pKP1	pKP1 with deletion of the full promoter region (PFull) created using primers oKP7/oKP8

Table 2. Primers used in this study

Primer	Sequence (5'-3')	Description
oSY1	GGCCAATAAGGCCTTTCTAGATT AAGAAATAATC	Forward primer for amplifying the pAJS23 plasmid
oSY2	GGCCTCGTTGGCCGTCGAC	Reverse primer for amplifying the pAJS23 plasmid
oKP1	GGTCGACGGCCAACGAGGCCTT GACCTTCTAACCCGCC	Forward primer for amplifying the *ctsR* repair template
oKP2	CTAGAAAGGCCTTATTGGCCGGT TTGCGGCTTTCATTG	Reverse primer for amplifying the *ctsR* repair template
oKP3	TAGAGCGATAAAGTCAAATATAG TCAAAGTCAGTAAAGGAG	Forward primer for ΔPA1
oKP4	TGACTTTATCGCTCTATCCTTCAT TATTTCCATTTTCCC	Reverse primer for ΔPA1
oKP5	ATTTTGGTTTAACTTTATACCGAA TTTTAAATCAGCAATCAGG	Forward primer for ΔPA2
oKP6	GTATAAAGTTAAACCAAAATACA AAAAACCCAGCTCATTG	Reverse primer for ΔPA2
oKP7	TTTTGGTTTTAAAGTCAAATATAG TCAAAGTCAGTAAAGGAGG	Forward primer for ΔPFull
oKP8	TTGACTTTAAAACCAAAATACAA AAAACCCAGCTCATTG	Reverse primer for ΔPFull
oFQ1	ATCGCTGGGTAGCTATGTGCG	Forward primer for PCR amplification of the promoter region
oFQ2	GTGCGTCCTGAATAAAATGCTTT AGCG	Reverse primer for PCR amplification of the promoter region
prRS9	GTGAAAAGTGGCTGGTCTCT	Reverse primer for Sanger sequencing of the promoter region

2-5 Isolating Chromosomal DNA

Chromosomal DNA from *B. subtilis* was extracted following the Camp Lab's "Isolating Genomic DNA" protocol, based on Promega's Wizard® Genomic DNA Purification Kit (Protocol III.G). A single isolated colony was inoculated into 3 mL of LB/Kan media and incubated at 37°C on a roller drum for approximately 4 hours. From this culture, 1.5 mL was transferred to a microcentrifuge tube and centrifuged at 13,000 x g for 2 minutes. The supernatant was discarded, and the remaining 1.5 mL of culture was processed in the same manner.

The cell pellet was resuspended in 480 µL of 50 mM EDTA, followed by the addition of 30 µL of 20 mg/mL lysozyme. The tubes were inverted to mix and incubated at 37°C for 60 minutes. Afterward, 600 µL of Nuclei Lysis Solution was added, and the sample was incubated at 80°C for 5 minutes to lyse the cells. The sample was then cooled to room temperature. 1.2 µL of 10 mg/mL RNase solution was added, and the solution was incubated at 37°C for 30 minutes before being cooled again.

Next, 200 µL of Protein Precipitation solution was added, and the mixture was vortexed for 20 seconds, resulting in a white precipitate and a decrease in viscosity. The sample was incubated on ice for 5 minutes, followed by centrifugation at 13,000 x g for 3 minutes. The supernatant (900 µL) was transferred to a new microcentrifuge tube containing 600 µL of room-temperature isopropanol, and the mixture was inverted gently until thread-like strands of DNA appeared. The sample was centrifuged again at 13,000 x g for 3 minutes. The liquid was carefully poured off, and the sample was centrifuged again at 13,000 x g for 2 minutes. After aspirating the remaining liquid, the pellet was air-dried for 20 minutes in the hood with the blower on and left uncapped overnight in a laminar flow hood to ensure complete drying. To

rehydrate the DNA, 100 µL of elution buffer was added, and the samples were incubated at 65°C for 1 hour. The DNA samples were then stored at -20°C.

The chromosomal DNA from the mutant isolates was subjected to PCR amplification using Taq polymerase and primers oFQ1/oFQ2 to amplify the promoter region. The resulting amplicons were sequenced to confirm the successful introduction of the intended mutations into the *B. subtilis* genome.

2-6 *B. subtilis* Strain Construction

2-6-1 Transformation into *B. subtilis*

DNA was transformed into B. subtilis using the "One-Step *B. subtilis* Transformation" protocol adapted by the Camp Lab (Wilson and Bott, 1968). A single colony of the recipient strain was inoculated into 3 mL 1× MC medium and incubated at 37°C in a roller drum for 4–5 hours to induce competence. The culture was then aliquoted into sterile tubes (200 µL each), and DNA was added to each tube, except the no-DNA control. The tubes were incubated at 37°C in a roller drum for 60–90 minutes. Following incubation, the entire volume from each transformation was plated onto selective LB agar plates and incubated overnight at 37°C. Colony growth on selective media indicated successful transformation.

2-6-2 Strain Construction by CRISPR-Cas9

Strain construction by CRISPR-Cas9 was carried out based on a previously described simplified protocol for *B. subtilis* (Sachla et al., 2021). pKP3, pKP4, and pKP5 plasmids were transformed into *B. subtilis ctsR::erm* (KPB5) using the adapted transformation protocol. Transformation mixtures were plated on LB agar containing 15 µg/mL kanamycin and 0.2% mannose (LB/Kan15/0.2% Mannose) and incubated overnight at 24°C to allow CRISPR editing.

Eight random colonies were selected and patched onto fresh LB/Kan15/0.2% Mannose plates. After overnight incubation at 24°C, colonies were repatched onto LB plates and incubated at 45°C to promote plasmid loss. After several rounds of repatching, colonies were screened for sensitivity to macrolide-lincosamide-streptogramin (MLS) and kanamycin. MLS sensitivity confirmed loss of the *erm* cassette (successful editing), and kanamycin sensitivity confirmed plasmid loss. Multiple single colonies were stored as glycerol stocks to retain multiple isolates of the mutated strain.

2-6-3 GFP-Strain Construction

Chromosomal DNA from the *clpC-gfp* reporter strain (BJK510; Kain et al., 2008) was transformed into the mutant strains (KPB6, KPB10, KPB16 and KPB17). Transformants were selected on LB/Kan5 plates and incubated overnight at 37°C. Twelve colonies were patched onto fresh LB/Kan5 plates, and four were selected for chromosomal DNA isolation. PCR (primers oFQ1/oFQ2) was used to confirm the presence of the GFP construct, and Sanger sequencing (primer prRS9) was used to verify that the promoter mutations were retained.

Table 3. *B. subtilis* strains used in this study

Strain	Genotype	Construction/Source
KPB1 (AHB1)	Wild type	Camp Strain Collection
KPB2 (AHB530)	Δ*clpC::erm*	Camp Strain Collection
KPB5 (KF215)	Δ*ctsR::erm*	Bacillus Genetic Stock Center's BKE Library
KPB6	ΔPA1-*clpC* Isolate 1	pKP3 → KPB5
KPB7	ΔPA1-*clpC* Isolate 2	pKP3 → KPB5
KPB10	ΔPA2-*clpC* Isolate 1	pKP4 → KPB5

KPB11	ΔPA2-*clpC* Isolate 2	pKP4 → KPB5
KPB13	ΔPFull-*clpC* Isolate 1	pKP5 → KPB5
KPB14	ΔPFull-*clpC* Isolate 2	pKP5 → KPB5
KPB15	ΔPFull-*clpC* Isolate 3	pKP5 → KPB5
KPB16	ΔPFull-*clpC* Isolate 4	pKP5 → KPB5
KPB17 (CGB8)	ΔPsigB/F amyE::PspoIIQ-*lacZ* cm Isolate 1 *	Chelsea Strain Collection
KPB18 (CGB9)	ΔPsigB/F amyE::PspoIIQ-*lacZ* cm Isolate 2 *	Chelsea Strain Collection
KPB19 (BJK510)	*clpC*ΩRBS-*gfp kan*	Kain et al. 2008
KPB21	ΔPA1-*clpC*ΩRBS-*gfp kan*	KPB19 chDNA → KPB6
KPB24	ΔPB/F-*clpC*ΩRBS-*gfp kan*	KPB19 chDNA → KPB17
KPB29	ΔPA2-*clpC*ΩRBS-*gfp kan*	KPB19 chDNA → KPB10
KPB33	ΔPFull-*clpC*ΩRBS-*gfp kan*	KPB19 chDNA → KPB16

* KPB17 and KPB18 contain a *lacZ* reporter at the amyE locus; not expected to affect results, but future studies should use a strain without the reporter.

2-7 Sporulation Assays

2-7-1 Sporulation by Nutrient Exhaustion

Sporulation was induced in *B. subtilis* strains by nutrient exhaustion using Difco sporulation medium (DSM) using a protocol developed by a previous Camp Lab member (Schaeffer et al., 1965). Strains were first streaked onto LB agar plates and incubated overnight at 37°C to obtain single colonies. On the following day, 100 mL of DSM was prepared and supplemented with 100 µL each of 100 mM $FeSO_4$, 1 M $Ca(NO_3)_2$, and 0.01 M $MnCl_2$ stock

solutions. Two milliliters of the supplemented DSM media were aliquoted into sterile culture tubes, and a single colony was inoculated into each tube. The cultures were incubated at 37°C in a roller drum for 24 hours.

After 24 hours, the cultures were heat-killed by placing them in a preheated 80°C water bath for 20 minutes to eliminate non-sporulating cells. The heat-treated cultures were allowed to cool on the bench for 10–20 minutes. 10-fold serial dilutions of the cultures were performed by transferring 111 µL of the heat-killed culture into 1 mL of sterile water up to 1e-6. The dilutions were vortexed and plated by spreading 100 µL of each dilution onto DSM agar plates using sterile glass beads. Plates were incubated overnight at 37°C.

The next day, colonies were counted on plates containing 30-300 colonies. Sporulation efficiency was calculated as: spores/mL = (colony count x dilution factor)/0.1, where 0.1 mL represents the plated volume. GraphPad Prism was then used to analyze and visualize the data.

2-7-2 Sporulation by Resuspension

Sporulation was induced by resuspension following a modified protocol from Harwood and Cutting (1990). *B. subtilis* strains were streaked onto LB agar plates and incubated at 37°C overnight. The following day, a single colony was inoculated into 3 mL of Casein Hydrolysate (CH) media and incubated at 37°C on a roller drum for 3 hours. The culture was then transferred to 1.5 mL microcentrifuge tubes and centrifuged at 13,000 x g for 1 minute. The supernatant was discarded, and the pellet was resuspended in an equal volume of Sterlini-Mandelstam (SM) Resuspension Media, which was prepared by mixing 90 mL of sporulation salts A + B, 5 mL of 1 M $MgSO_4$, 4 mL of 5% L-glutamic acid, and 1 mL of 0.1 M $CaCl_2$. The culture was incubated at 37°C on a roller drum for an additional 3 hours.

2-8 Microscopy

Cells were harvested at hour 3 of sporulation after induction by resuspension. 200 µL of culture was centrifuged at 13,000 × g for 1 minute, and the supernatant was discarded. The pellet was resuspended in 20 µL of 5× FM 4-64 dye in 1× PBS.

A 3% low-melting point (LMP) agarose solution was heated to 65°C. 50 µL was placed on a glass slab and covered with a glass slide to form a pad. Once set, 2 µL of the stained cell suspension was mounted on the agarose pad and covered with a Poly-L-lysine coated coverslip.

The cells were imaged using a Nikon Eclipse Ti microscope equipped with Chroma filter sets 49002 (GFP) and 49017 (FM 4-64). Images were captured using an Orca-Flash4.0 Digital CMOS camera and NIS-Elements Advanced Research software (v4.30.02, Nikon Instruments Inc.). Exposure times were consistent across samples: 500 ms for GFP, 700 ms for Texas Red, and 1 s for Phase contrast. BJK510 was included as a control on each imaging day.

2-9 Image Processing and Data Analysis

Fluorescence microscopy images were processed using the Fiji ImageJ software. Brightness and contrast were adjusted in the Texas Red channel as needed, while GFP channel settings were kept constant. Individual cells for result analysis were selected randomly based on sporulation stage, identified using membrane fluorescence, with GFP signal revealed only after selection to avoid bias.

Fluorescence intensity across the forespore–mother cell axis in fully engulfed cells was quantified using the Plot Profile tool in ImageJ. The data was then processed using Excel and RStudio (v2023.06.2 +561). First, x-values were normalized to relative distance from the forespore pole to account for size differences between cells. Data wrangling and interpolation were performed using the “dplyr,” “splines,” and “tidyr” packages. Specifically, normalized

x-values and corresponding intensities were used with the ‘spline’ function to interpolate intensity values at every 0.02 interval. The interpolated intensity data from individual cells were then averaged to generate mean intensity profiles. Final plots were created using Excel and GraphPad Prism. Sample R code can be found in the appendix.

CHAPTER 3: RESULTS

3-1 Generation of Promoter Deletion Mutants

To investigate the transcriptional regulation of the *clpC* operon, I focused on the upstream promoter region containing predicted sigma factor binding sites. Using previously identified consensus sequences, I targeted three distinct promoter regions—two associated with σ^A and one overlapping site recognized by both σ^B and σ^F. To examine their individual and combined roles in operon expression, I characterized four CRISPR-Cas9-based promoter deletion mutants: three targeting each specific binding site (denoted ΔPA1, ΔPB/F and ΔPA2), and one spanning the entire promoter region (ΔPFull). The ΔPB/F mutant was constructed previously by a colleague, while the remaining three mutants were designed, cloned, and validated as part of this study.

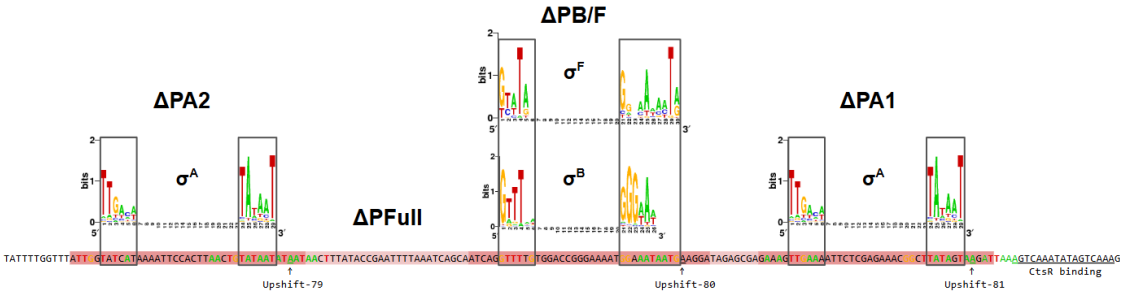

Figure 10. Sigma factor consensus sequences and targeted deletions in the *clpC* promoter region. Diagram showing the three upstream promoter regions of the clpC operon with their predicted sigma factor consensus sequences. Dark red boxes indicate the sequences deleted in each single promoter mutant (PA2, PB/F, and PA1, left to right). The light red box represents the larger region deleted in the triple promoter mutant (ΔPFull).

CRISPR technology provided a precise and efficient tool for these deletions, enabling the targeted modification of specific regions. For this study, I adapted the simplified CRISPR system for *B. subtilis* described by Sachla et al. (2021), which utilizes the BKE strain library, a pre-existing collection of almost 4,000 *B. subtilis* strains with individual genes replaced by an erythromycin (*erm*) resistance cassette. This system also employs the pAJS23 plasmid, which

encodes an erm-specific guide RNA, Cas9, and a Kanamycin resistance marker. Together, these tools allowed me to target a specific locus simply by selecting an appropriate *erm*-replacement strain and using the pAJS23 plasmid for genome editing.

For homologous recombination, I selected the *ctsR* gene, located adjacent to the promoter region, as the basis for our repair template. A repair template containing *ctsR* and sufficient upstream and downstream flanking regions was inserted into the pAJS23 plasmid using a PCR-based FastCloning method (Li et al., 2011), followed by site-directed mutagenesis to introduce the desired promoter deletions (Liu and Naismith, 2008) (Figure 11a).

The engineered plasmids were transformed into the *ctsR::erm* strain, and transformants were selected and grown under conditions that induced mannose-dependent expression of Cas9 and the *erm*-guide RNA. Cas9-mediated cleavage at the *ctsR* locus, directed by binding of the guide RNA to the *erm* cassette, prompted the cells to repair the double-strand break using the modified repair template, thereby incorporating the intended promoter deletions into the genome (Figure 11b). Throughout this process, it was critical to ensure that recombination occurred upstream of the promoter region to successfully introduce the desired deletions. Proper insertion and sequence accuracy were confirmed by PCR screening and DNA sequencing at multiple stages.

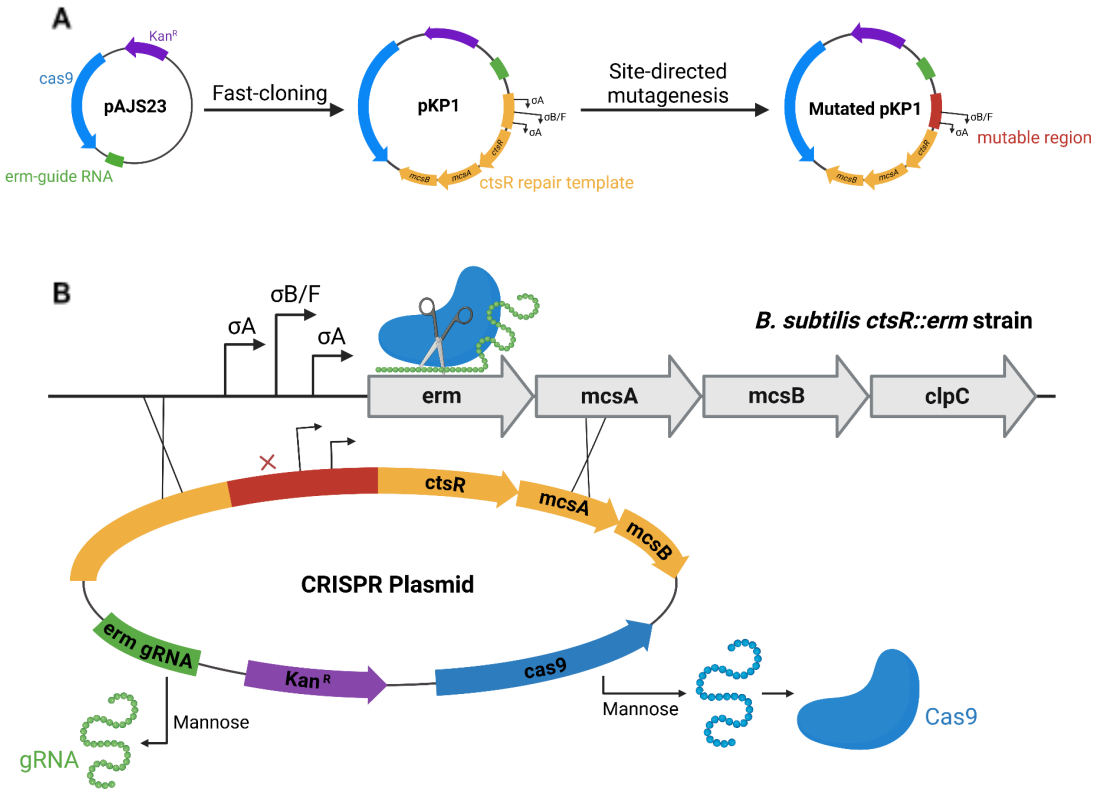

Figure 11. Overview of the CRISPR-Cas9 strategy used to generate *clpC* promoter deletion mutants in *B. subtilis*. (A) Diagram of the cloning and mutagenesis workflow used to construct CRISPR-Cas9 plasmids containing specific promoter deletions. (B) Schematic of the CRISPR-Cas9 editing process in *B. subtilis*, where the Cas9-gRNA complex introduces a double-strand break in the *erm* gene at the *ctsR* locus near the promoter region, and the mutation is incorporated via homologous recombination using the provided repair template (made using BioRender).

3-2 *clpC-gfp* Reporter Reveals Promoter-Specific Expression Patterns

To assess how each promoter influences *clpC* expression, I introduced a transcriptional *clpC-gfp* reporter into each mutant background. This reporter was inserted directly downstream of the *clpC* gene and is expressed whenever *clpC* is transcribed. Green fluorescence therefore directly reflects *clpC* expression levels. Fluorescence microscopy of sporulating cells revealed distinct differences in expression patterns across the promoter deletion strains, suggesting that each promoter plays a unique regulatory role (Figure 12 and Figure 13).

To broadly visualize how the promoter deletions affect *clpC* expression, imaging was performed across consistent fields of view with fixed dimensions that included cells at various stages of sporulation. Figure 12 presents representative phase contrast, Texas Red membrane stain, and GFP fluorescence images for each strain, allowing qualitative comparison of *clpC* expression levels across a fixed spatial scale.

In the wild-type strain, I observed moderate GFP signal in vegetative cells and a marked increase in fluorescence in the forespore as sporulation progressed, consistent with known regulation of the *clpC* operon (Kain et al., 2008). In the ΔPA1 mutant, which lacks the downstream σ^A binding site, I observed a pronounced reduction in GFP intensity in the mother cell and in vegetative cells, suggesting that this promoter contributes to both sporulation-specific and baseline transcription. In contrast, the ΔPB/F mutant, lacking the forespore-specific σF binding site, exhibited loss of forespore-specific GFP while maintaining normal mother cell expression, indicating that this promoter is responsible for activating *clpC* post-septation in the forespore. The ΔPA2 mutant, lacking the upstream σ^A site, displayed GFP levels nearly identical to wild type in both vegetative and sporulating cells, suggesting that this promoter is either inactive under the conditions tested or functionally redundant. Finally, the ΔPFull mutant, in which the entire promoter region was deleted, exhibited barely detectable fluorescence levels in all cell types and sporulation stages, suggesting that the deleted regions are collectively essential for *clpC* transcriptional activity.

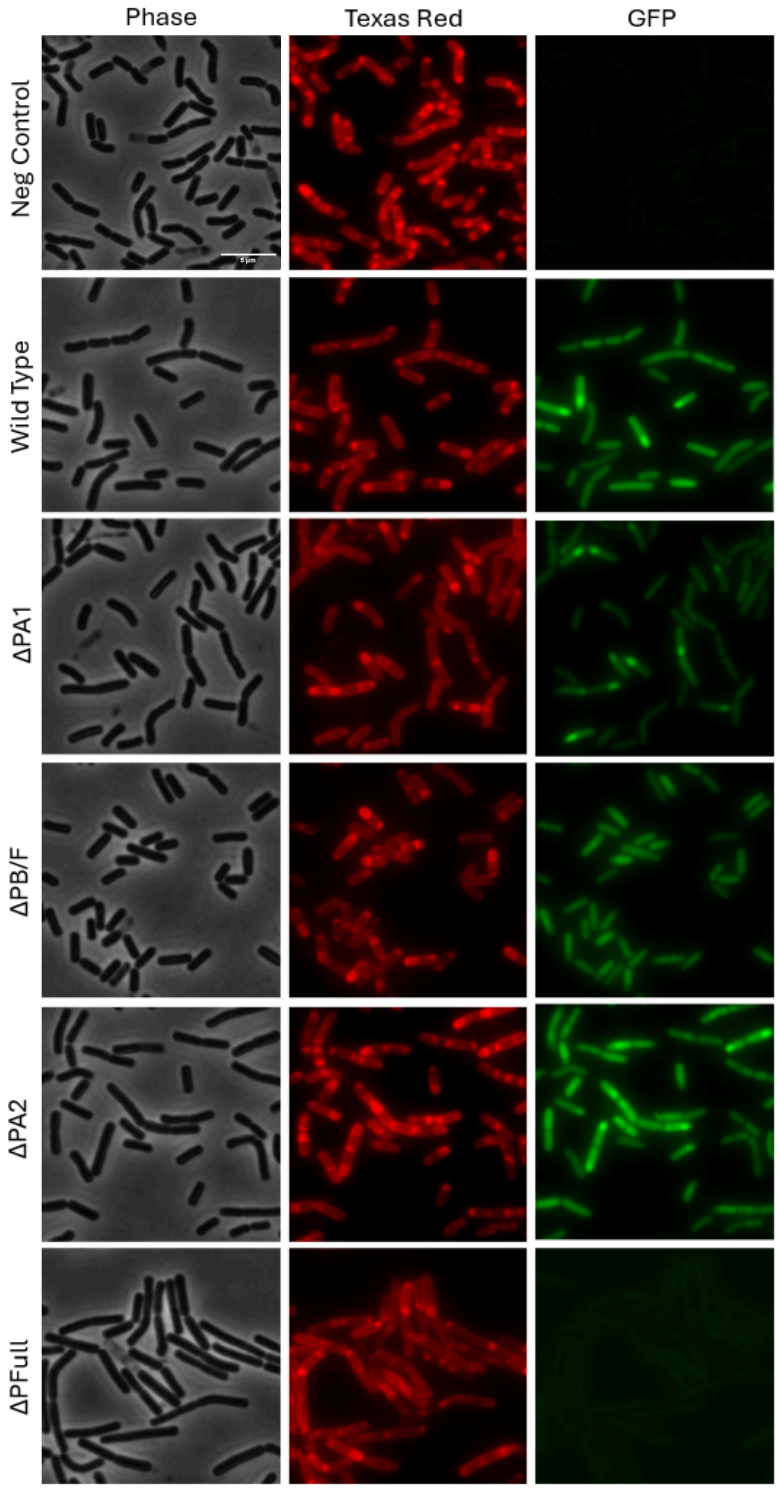

Figure 12. Representative images of *clpC* promoter mutants and control strains during sporulation. Phase contrast, Texas Red membrane staining, and GFP fluorescence images were captured using fixed fields of view (500x500 pixels) to enable direct comparison of *clpC* expression patterns across strains. The strains shown, listed from top to bottom, are: KPB1, KPB19, KPB21, KPB24, KPB29, and KPB33.

3-2-1 Sporulation Stage Specific Changes in *clpC* Expression

To understand how *clpC* expression changes throughout sporulation, I imaged individual cells from each strain at five defined stages—vegetative, polar septation, early engulfment, late engulfment, and post-engulfment (Figure 13). GFP and Texas Red fluorescence were used to monitor expression and compartment identity across stages.

During vegetative growth, the wild-type strain showed baseline fluorescence, which was reduced in ΔPA1 and nearly undetectable in ΔPFull. Other strains resembled wild-type. Following polar septation, compartmentalization of expression became clearer. Mother cell expression persisted in the wild-type and all the mutants except ΔPA1, which remained dimmer. The ΔPB/F strain exhibited a noticeable drop in forespore signal relative to the mother cell, consistent with the role of the σ^F-dependent promoter in activating forespore transcription. ΔPFull remained low across both compartments.

In early engulfment, forespore fluorescence began to increase in wild-type, ΔPA1, and ΔPA2, while ΔPB/F forespores remained dim and ΔPA1 mother cell signal stayed low. ΔPFull continued to show little to no expression. This trend held in late engulfment: forespore signals further intensified in wild-type, ΔPA1, and ΔPA2, while ΔPB/F forespores stayed dimmer and ΔPA1 mother cells remained relatively dark. Expression in ΔPFull remained very faint.

By post-engulfment, forespore expression peaked in wild-type, ΔPA1, and ΔPA2 strains. ΔPA1 showed a slight increase in mother cell signal over the course of sporulation, though it remained weaker overall. ΔPB/F forespores remained dim, and ΔPFull cells continued to show minimal fluorescence.

Overall, these results highlight the stage- and compartment-specific contributions of each promoter. PA1 is important for both vegetative and mother cell expression, PB/F is critical for

forespore-specific activation, and the absence of all upstream promoters in the ΔPFull mutant nearly eliminates *clpC* transcription.

Figure 13. Temporal and compartment-specific *clpC* expression across the mutant strains. Images of five randomly selected cells per strain were captured at each defined sporulation stage—vegetative, polar septation, early engulfment, late engulfment, and post-engulfment—using Texas Red membrane staining and GFP fluorescence to visualize *clpC* expression. All images for each strain were obtained from a single slide preparation on the same day. Strains shown from top to bottom are: KPB19, KPB21, KPB24, KPB29, and KPB33.

3-2-2 Quantitative Analyses of *clpC* Expression Based on Fluorescence Intensities

To quantify GFP expression and assess compartment-specific activity across strains, I measured fluorescence intensity along the forespore-to-mother cell axis in ten fully engulfed sporulating cells per strain (Figure 14). The post-engulfment stage was selected because *clpC* expression peaks during this phase.

In the wild-type strain, forespore intensity ranged from ~17,500–22,500, while mother cell levels were ~12,500, with one outlier reaching ~16,000. In the ΔPA1 mutant, mother cell expression dropped significantly (~7,500), and forespore levels showed a mild reduction (~12,500–17,500). The ΔPB/F mutant showed a drastic reduction in forespore intensity (~7,500–10,000), while mother cell expression (~12,500) remained comparable to wild-type. ΔPA2 displayed more variable expression with modest drops in both compartments in some cells. The ΔPFull strain showed consistently low expression (<7,500), only slightly above background levels (~5,000) measured in the negative control (Figure 14).

To summarize these trends, I averaged the GFP intensity profiles for each strain to generate composite traces (Figure 15). The averaged data reinforce that ΔPA1 significantly reduces mother cell expression and moderately lowers forespore expression. ΔPB/F causes a sharp decrease in forespore expression while mother cell expression remains similar to wild type. ΔPA2 results in a slight drop in forespore expression, with little to no change in the mother cell. ΔPFull reduces expression in both compartments, with a slightly greater reduction in the forespore.

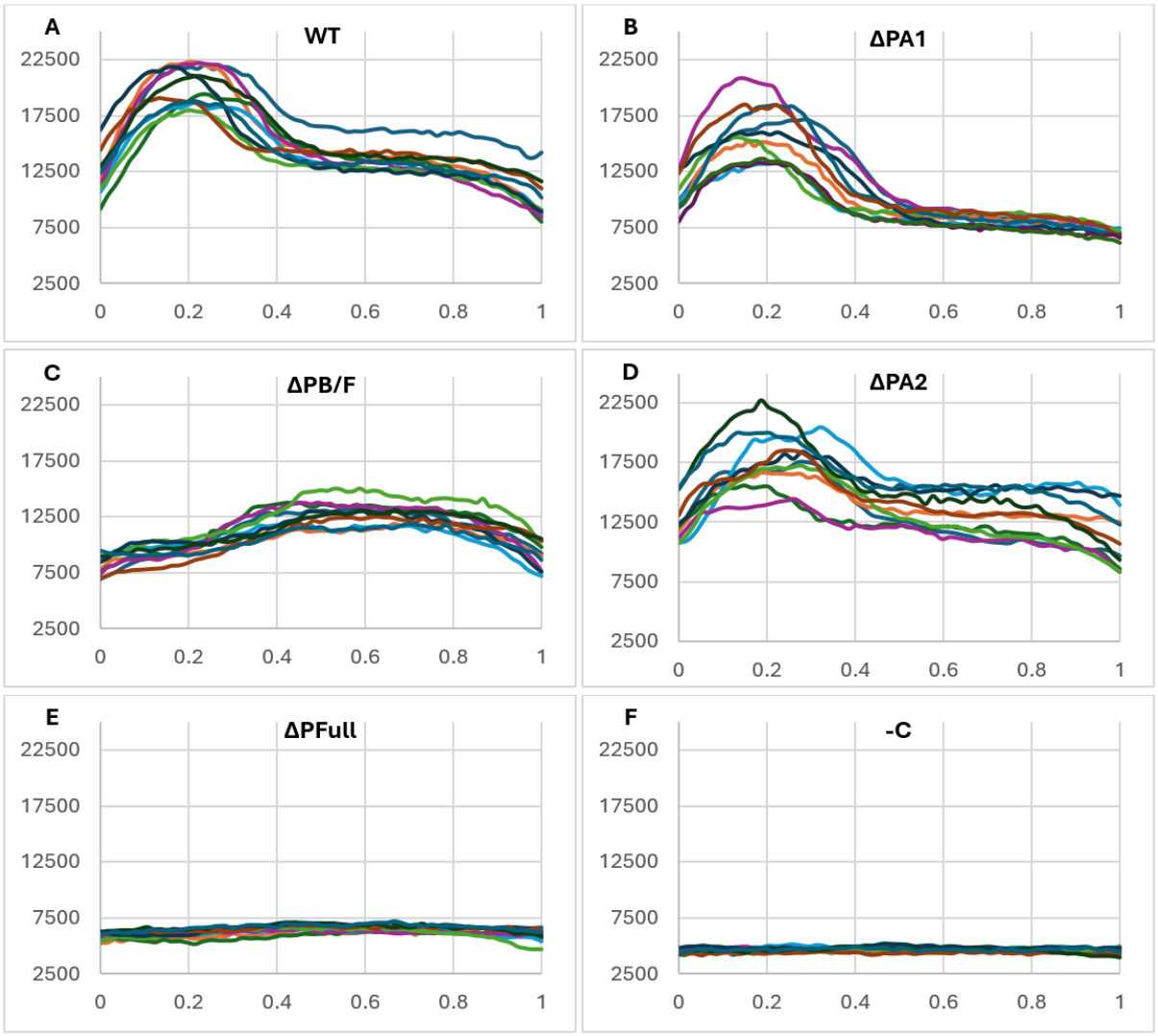

Figure 14. Spatial profiles of *clpC* expression in fully engulfed cells. Panels A–F show GFP intensity plots across the horizontal axis of fully engulfed sporulating cells (n = 10), from the forespore (left, ~0 to 0.4) to the mother cell (right, ~0.4 to 1). Expression profiles illustrate compartment-specific differences in *clpC* activity across strains. Each panel corresponds to a different strain: (A) KPB19, (B) KPB21, (C) KPB24, (D) KPB29, (E) KPB33, and (F) KPB1.

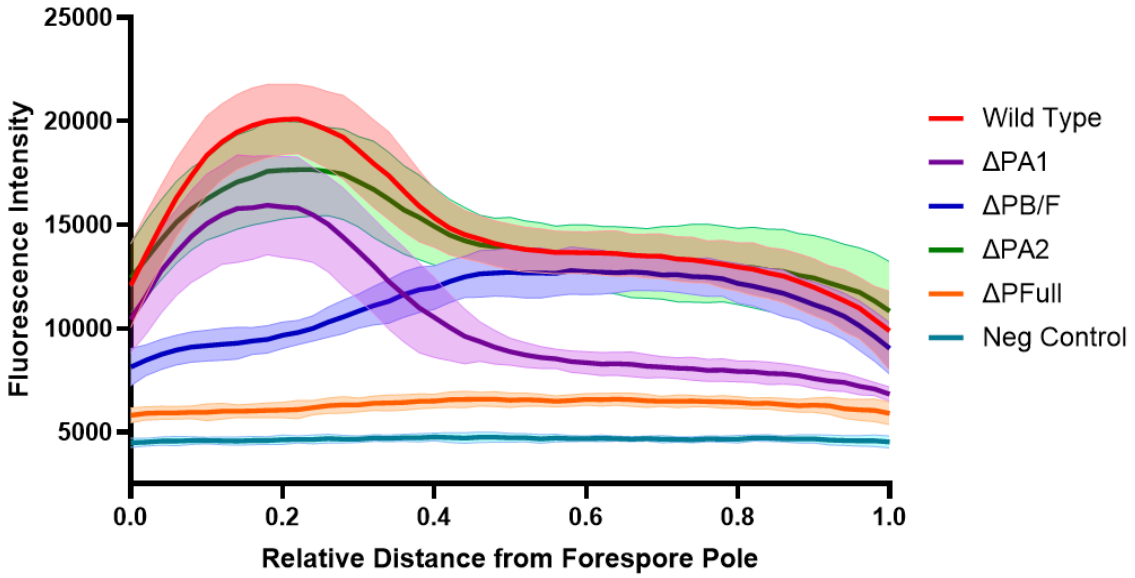

Figure 15. Averaged *clpC* expression profiles in fully engulfed cells across each strain. Line graphs show mean GFP intensity along the horizontal axis from forespore (left, ~0 to 0.4) to mother cell (right, ~0.4 to 1), averaged from ten fully engulfed cells per strain. Profiles compare spatial expression patterns between wild-type (KPB19), promoter deletion mutants (KPB21, KPB24, KPB29 and KPB33), and the negative control (KPB1). Lighter shading represents one standard deviation above and below the mean.

3-3 Promoter Deletions Do Not Significantly Reduce Sporulation Efficiency

To determine whether the loss of specific *clpC* promoters affected the overall ability of cells to complete sporulation, I induced sporulation via nutrient exhaustion and subsequently subjected the cultures to heat shock to eliminate vegetative cells. Heat-resistant colony-forming units (CFUs) were then quantified to assess spore formation efficiency (Figure 16).

Consistent with previous findings in the lab, the Δ*clpC* mutant strain, which entirely lacks the *clpC* gene, showed a dramatic reduction—approximately four orders of magnitude—in sporulation efficiency compared to the wild-type control. This result reflects the essential role of *clpC* in the sporulation process. In contrast, the ΔPA1, ΔPB/F, and ΔPA2 single promoter deletion strains exhibited no significant reduction in sporulation efficiency. Both unique isolates

of all three mutants produced heat-resistant spores at concentrations of approximately 10^8 CFU/mL, which were comparable to wild-type levels. The ΔPFull strain, which lacks all three targeted promoter regions, did not fully replicate the severe sporulation defect observed in the Δ*clpC* mutant but did exhibit greater variability in sporulation efficiency across biological isolates. One isolate in particular, KPB14, yielded inconsistent results—sometimes showing wild-type levels and other times showing a one- to three-order-of-magnitude reduction—indicating that while deletion of a single promoter does not compromise spore production, the combined loss may partially disrupt sporulation efficiency.

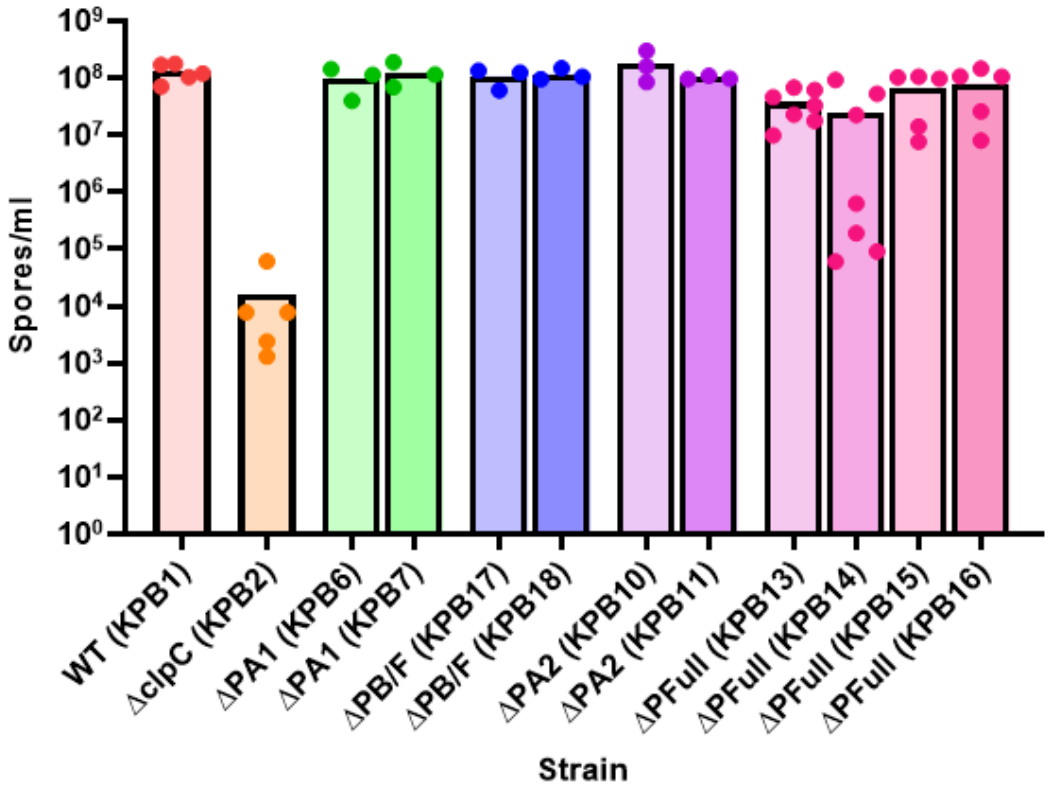

Figure 16. Sporulation efficiency of *clpC* promoter deletion mutants. Bar graph showing spores/mL for wild-type, Δ*clpC*, and the promoter deletion mutants. Two independently constructed isolates were included for each single promoter mutant and four isolates were included for the full promoter mutant. Each data point represents a separate biological replicate from an individual colony, with experiments performed on different days. The Δ*clpC* strain exhibited a pronounced sporulation defect, while single promoter deletions did not significantly affect sporulation efficiency. ΔPFull isolates displayed variable phenotypes, suggesting potential genetic heterogeneity or compensatory mechanisms.

CHAPTER 4: DISCUSSION

ClpC plays a critical role in the initiation and progression of sporulation by degrading key regulatory proteins such as SpoIIAB, as well as other enzymes and transcription factors essential for both initiating and sustaining sporulation (Riley et al., 2025; Pan et al., 2001). The Camp Lab has been investigating the transcriptional regulation of the *clpC* operon for several years, with prior student research helping shape the current model (Berg, 2023; Quigley, 2023; Mayangsari, 2018; Nkomboni, 2017).

Based on previous literature and biochemical analysis of predicted sigma factor consensus sequences, there is strong evidence that the σ^A promoter directly upstream of *ctsR*, as well as σ^B and σ^H-dependent promoters, are active (Nkomboni, 2017; Krüger et al., 1996; Krüger et al., 1994). Unpublished data also suggest that the σ^B-dependent promoter shares a consensus sequence with σ^F. Additionally, transcriptomic data from Nicolas et al. (2012) identified a second σ^A promoter located further upstream. This promoter had not been previously tested or validated in our lab and remains largely uncharacterized in the literature, representing a new regulatory element in the *clpC* operon.

This study aimed to clarify the contributions of these upstream sigma factor-dependent promoters in regulating *clpC* expression during sporulation in *B. subtilis*. Using a CRISPR-based approach, I dissected promoter activity across cellular compartments and sporulation stages. Our findings demonstrate that *clpC* expression is regulated by multiple sigma factor-dependent promoters, each active at different sporulation stages and in different cellular compartments. Microscopy analysis indicates that the PA1 promoter primarily drives *clpC* expression in the mother cell, while the PB/F promoter is responsible for expression in the forespore. Moreover, removing all three promoters results in a drastic decrease in *clpC* levels throughout the cell.

However, despite these reductions neither the individual promoters nor the full promoter region deletion, are sufficient to impair the cell's ability to successfully undergo sporulation. This suggests that *clpC* expression is maintained through redundant regulatory mechanisms and that only low levels of *clpC* are needed for sporulation to occur. These findings highlight the robustness of *clpC* regulation and suggest that additional promoter elements or compensatory pathways may also be involved.

4-1 PA1 is Primarily Responsible for *clpC* Expression in the Vegetative and Mother Cell

The σ^A-dependent promoter (PA1), located directly upstream of the *clpC* operon, plays a key role in regulating *clpC* expression during both vegetative growth and sporulation in *B. subtilis*. Previous studies have shown that PA1 is active under non-stress conditions and can compensate for the σ^B promoter in its absence, maintaining *clpC* induction in response to stressors like heat and ethanol (Krüger et al., 1996).

Our fluorescence microscopy and quantitative analyses confirm the importance of PA1 in regulating *clpC* expression. Deletion of this promoter results in a significant reduction in *clpC* expression in the mother cell throughout all stages of sporulation, as well as in non-sporulating cells. This aligns with the known function of σ^A as the primary sigma factor during vegetative growth, as well as indicates an important role in mother cell specific expression of *clpC*.

The transcriptomic data from Nicolas et al. (2012) further supports this, suggesting that *clpC* expression from PA1 is high during the early stages of sporulation but gradually decreases, plateauing around hour 3 (Dérozier et al., 2021). This trend mirrors the declining availability of σ^A-bound RNA polymerase over time; by hour 3, the proportion of σ^A associated with core RNA polymerase drops from ~50% at the onset of sporulation to less than 10% (Ju et al., 1999).

In the PA1 deletion mutant, reduced *clpC* expression in the forespore likely reflects lower transcript levels inherited from the vegetative state, where PA1-driven transcription is compromised. Although the σ^B/σ^F-dependent promoter remains functional in this mutant, facilitating *clpC* expression in the forespore, the initial deficit from impaired vegetative expression results in overall lower *clpC* levels compared to the wild type. Meanwhile, the mother cell is unable to compensate for the loss of PA1, leading to a more pronounced reduction in *clpC* expression in this compartment.

These findings highlight the critical role of PA1 in establishing adequate *clpC* levels during vegetative growth, as well as the compartment-specific regulation of *clpC* expression in the mother cell.

4-2 PB/F is Primarily Responsible for *clpC* Expression in the Forespore

Microscopy analysis of the σ^B/σ^F mutant strain reveals a significant reduction in forespore fluorescence, indicating that the σ^B/σ^F-dependent promoter is essential for *clpC* expression in this compartment. This observation aligns with the established roles of σ^F and σ^B in *B. subtilis*. σ^F is the first compartment-specific sigma factor activated during sporulation, directing early forespore gene expression, while σ^B is a general stress response sigma factor that becomes active under various stress conditions, including those encountered during sporulation (Carniol et al. 2004; Pan and Losick, 2003; Krüger et al., 1994).

Previous studies have shown a boost in *clpC* expression specifically in the forespore, which was hypothesized to be driven by σ^F, but this hadn't been directly tested (Kain et al. 2009). Our data now supports that hypothesis, providing evidence that the σ^F-dependent promoter is indeed responsible for this forespore-specific increase.

The diminished *clpC* expression in the forespore of the σ^B/σ^F mutant suggests that either one or both sigma factors contribute to its expression in the forespore. Given that σ^F is specifically activated in the forespore, it likely plays a direct role in initiating *clpC* expression there. σ^B may also influence *clpC* expression indirectly by modulating stress response pathways intersecting with sporulation processes. For instance, σ^B has been shown to induce the expression of Spo0E, an aspartyl-phosphatase that dephosphorylates Spo0A~P, thereby affecting sporulation initiation (Rodriguez Ayala et al., 2020; Reder et al., 2012). However, as mentioned earlier, previous studies have shown that the downstream σ^A can compensate for σ^B under stressful conditions, which suggests that the *clpC* defect in the forespore might be primarily due to the absence of the σ^F promoter (Krüger et al., 1996). Overall, this regulatory interplay highlights the integration of stress responses with developmental programs in *B. subtilis* and the need for further experimentation to fully dissect the distinct contributions of σ^B and σ^F to *clpC* regulation.

Notably, some cells in the ΔPB/F mutant also exhibit increased *clpC* expression in the mother cell, as seen in the microscopy images. While our present data and the average intensity quantification are not sufficient to confirm this as an actual phenotypic difference, further analysis is needed. However, it is possible that σ^B has some contribution to expression either in the vegetative cell just before sporulation initiation or in the mother cell and its loss leads to compensatory activation of σ^A-dependent promoters, resulting in elevated *clpC* expression in the mother cell (Krüger et al., 1996). This would align with σ^B's role as a general stress response factor, which becomes active when cells encounter environmental stressors like those encountered during sporulation induction (Rodriguez Ayala et al., 2020). This potential compensatory mechanism highlights the redundancy of regulatory networks governing *clpC* expression during sporulation.

4-3 PA2 Does Not Play a Major Role in *clpC* Expression During Sporulation

Microscopy analysis of the ΔPA2 mutant strain shows that deletion of the upstream σ^A-dependent promoter does not result in a significant reduction in *clpC* expression during either sporulation or vegetative growth. This suggests that while the PA2 promoter may contribute to *clpC* expression, it is not essential for robust expression during sporulation. However, increased variability in fluorescence among individual cells suggests that compensatory mechanisms might be activated to maintain *clpC* expression levels.

Transcriptomic studies have demonstrated that PA2 is active during sporulation, with a transcription upshift detected directly downstream the promoter site (Dérozier et al., 2021; Nicolas et al., 2012). The absence of a strong phenotype upon PA2 deletion is therefore surprising and suggests that its function may be redundant. One possibility is that the downstream σ^A-dependent promoter (PA1) is the primary σ^A-dependent promoter for the operon and can compensate for the loss of PA2, maintaining sufficient *clpC* expression in its absence. Alternatively, PA2 might play a role under specific conditions or developmental stages not captured in our experimental setup.

Therefore, while PA2 may have a supporting role, it does not appear to be a major driver of *clpC* expression during sporulation under the conditions tested. Since not much is known about this promoter, further experiments, such as time-course expression analyses or different stress induction assays, might be helpful in clarifying the specific contexts in which PA2 becomes more functionally relevant.

4-4 Promoter Mutations Do Not Cause a Significant Sporulation Defect

Sporulation assays under nutrient exhaustion conditions indicate that individual promoter mutations within the *clpC* operon do not substantially impact sporulation efficiency. Mutants

lacking the downstream σ^A-dependent promoter, the σ^B/σ^F-dependent promoter, or the upstream σ^A-dependent promoter all exhibited spore formation levels comparable to the wild-type strain. This suggests a level of functional redundancy within the regulatory system, where alternative promoters or regulatory mechanisms can compensate for the loss of any single promoter. This is in line with the compensatory effects that have been previously reported (Krüger et al., 1996).

Interestingly, the full promoter mutant, which lacks all three promoters and shows a drastic reduction in overall *clpC* expression, does not fully recapitulate the sporulation defect observed in a Δ*clpC* strain. Instead, it displays a more variable phenotype. Among four independently constructed ΔPFull isolates, one exhibited distinct variations in spore formation, suggesting a partial defect. This variability suggests that additional regulatory mechanisms or genetic adaptations, such as suppressor mutations, may mitigate the effects of complete promoter loss.

Suppressor mutations are a well-documented phenomenon in *B. subtilis*, especially under sustained stress or selective pressure (Tevethia et al., 1974). In this study, cells were grown overnight in DSM medium—a nutrient-poor condition known to impose prolonged stress prior to sporulation initiation (Schaeffer et al., 1965). Such conditions may have favored the emergence of secondary mutations that restored expression of *clpC* or activated compensatory pathways, allowing the cells to adapt. Additionally, because the promoter region controls the expression of the entire operon, deletion may have disrupted expression of *ctsR* and *mcsB*, two genes critical for protein quality control and stress survival (Fuhrmann et al., 2009; Kirstein et al., 2005). Disruption of their expression could also trigger compensatory genetic changes that indirectly rescue sporulation capacity.

Furthermore, ΔPFull mutants showed delayed colony formation post-transformation, requiring an additional 24–48 hours to recover on selective media. This observation suggests that these strains initially suffered from growth or fitness defects that were later compensated, potentially by suppressor mutations, which were then inherited by subsequent generations. Since each ΔPFull isolate was independently constructed, distinct suppressor mutations possibly arose in each strain during recovery, explaining the phenotypic variation.

The persistence of some *clpC* expression in ΔPFull mutants also raises the possibility that uncharacterized promoter elements exist. The σ^H-dependent promoter located in the *mcsB* gene has been previously suggested to contribute to expression of the operon, and since this promoter was not deleted in the ΔPFull construct, it may account for the residual *clpC* expression (Nkomboni, 2017).

Finally, other proteases such as ClpP in complex with alternative ATPases (e.g., ClpE or ClpX) might compensate for the loss of ClpC during sporulation, as protein degradation is a tightly regulated and redundant process in *B. subtilis* (Kirstein et al., 2008; Miethke et al., 2006; Gerth et al., 2004).

4-5 Limitations and Future Directions

This study has several limitations that may impact the interpretation and generalizability of the results. Due to time constraints, only one isolate per strain was used to generate the GFP reporter strains. This is particularly relevant for the full promoter mutant (ΔPFull), where each isolate exhibited distinct phenotypes. Constructing GFP fusions in additional isolates is necessary to verify the consistency of the observed phenotypes across different genetic backgrounds.

Moreover, all the microscopy for each strain was conducted on a single day. Although appropriate controls were included, this approach does not account for potential day-to-day variations in experimental conditions or biological responses. To mitigate this, future studies should incorporate multiple slide preparations and microscopy sessions across different days to ensure reproducibility and account for temporal variability.

The possibility of suppressor mutations also highlights the need for cleaner genetic manipulation strategies. Introducing the ΔPFull construct into a fresh background via congression—a process in *B. subtilis* where a specific DNA fragment is introduced into the chromosome during natural competence by co-transforming the high concentrations of donor DNA with a selectable marker (Zeigler et al., 2008). This could help minimize unintended secondary mutations that may have been acquired during earlier strain construction steps. This could subsequently help reveal the true phenotype of the ΔPFull mutant.

Additionally, while the DSM-based sporulation assay is well-established, it may not be ideal for evaluating mutants with impaired stress tolerance. DSM promotes asynchronous and prolonged sporulation under severe nutrient limitation, which can exacerbate growth or sporulation defects in sensitive strains like ΔPFull. The extended incubation and subsequent heat shock also increase the chance for spontaneous suppressor mutations that artificially rescue phenotypes. To better assess sporulation efficiency, alternative assays such as sporulation by resuspension—which induces synchronous sporulation in nutrient-limited medium at a defined time point—should be explored. This quicker and more controlled method could provide a more accurate reflection of the sporulation capabilities of each mutant and reduce selection for suppressors.

Furthermore, CRISPR-Cas9 was used to precisely generate promoter mutations and while the targeted regions were sequenced to confirm successful editing, off-target effects remain a concern. Unintended edits elsewhere in the genome could affect gene expression or phenotype in ways not accounted for. Future studies might use whole-genome sequencing or high-fidelity Cas9 variants to minimize this concern (Kleinstiver et al., 2016). In addition, the mutagenesis strategy used in this study was relatively aggressive, involving complete deletion of promoter regions. As previously discussed, this approach not only removes regulatory elements but may also affect adjacent critical genes and alter mRNA transcript length, potentially impacting post-transcriptional and post-translational stability (Bregman et al., 2011; Fuhrmann et al., 2009; Kirstein et al., 2005). Future studies could consider alternative strategies, such as scrambling key promoter motifs or introducing specific point mutations, to disrupt promoter recognition without removing large sections of DNA.

Finally, while this study provides important preliminary insights into the transcriptional regulation of *clpC*, more work is needed to dissect the functional roles of individual promoter regions. Constructing and analyzing double mutants, such as ΔPA1–ΔPA2 or ΔPA1–ΔPB/F, could clarify whether different promoter regions contribute independently or cooperatively to *clpC* expression. In particular, a ΔPA1–ΔPB/F mutant may reveal whether PA2 alone drives any *clpC* expression.

The potential role of the σ^H-dependent promoter also needs to be explored. Generating a ΔPFull–ΔPH double mutant would help test whether this alternative promoter accounts for the low-level expression still seen in the ΔPFull background. If removing the σ^H promoter eliminates all detectable *clpC* expression, this would suggest that all functionally relevant promoters have been identified. Additionally, if the sporulation phenotype in the ΔPFull–ΔPH strain remains

similar to that of ΔPFull, it would suggest that the residual expression was not sufficient for normal function and that suppressor mutations or compensatory pathways may be involved. This would help distinguish between minimal *clpC* expression maintaining sporulation and alternative genetic mechanisms rescuing the phenotype.

Collectively, addressing these limitations and expanding on the current findings will strengthen our understanding of how *clpC* expression is controlled and how its regulation impacts sporulation and stress response in *B. subtilis*.

REFERENCES

Aljghami, M. E., Barghash, M. M., Majaesic, E., Bhandari, V., & Houry, W. A. (2022). Cellular functions of the ClpP protease impacting bacterial virulence. *Frontiers in Molecular Biosciences*, *9*. https://doi.org/10.3389/fmolb.2022.1054408

Berg, A, (2023). Investigating expression of the AAA+ protease component clpC in the developing Bacillus subtilis spore. Mount Holyoke College.

Bradshaw, N., & Losick, R. (n.d.). Asymmetric division triggers cell-specific gene expression through coupled capture and stabilization of a phosphatase. *eLife*, *4*, e08145. https://doi.org/10.7554/eLife.08145

Bregman, A., Avraham-Kelbert, M., Barkai, O., Duek, L., Guterman, A., & Choder, M. (2011). Promoter Elements Regulate Cytoplasmic mRNA Decay. Cell, 147(7), 1473–1483. https://doi.org/10.1016/j.cell.2011.12.005

Camp, A. H., & Losick, R. (2009). A feeding tube model for activation of a cell-specific transcription factor during sporulation in Bacillus subtilis. *Genes & Development*, *23*(8), 1014–1024. https://doi.org/10.1101/gad.1781709

Carniol, K., Eichenberger, P., & Losick, R. (2004). A Threshold Mechanism Governing Activation of the Developmental Regulatory Protein σF in *Bacillus subtilis**. *Journal of Biological Chemistry*, *279*(15), 14860–14870. https://doi.org/10.1074/jbc.M314274200

Choules, M. P., Wolf, N. M., Lee, H., Anderson, J. R., Grzelak, E. M., Wang, Y., Ma, R., Gao, W., McAlpine, J. B., Jin, Y.-Y., Cheng, J., Lee, H., Suh, J.-W., Duc, N. M., Paik, S., Choe, J. H., Jo, E.-K., Chang, C. L., Lee, J. S., … Cho, S. (2019). Rufomycin Targets ClpC1 Proteolysis in Mycobacterium tuberculosis and M. abscessus. *Antimicrobial Agents and Chemotherapy*, *63*(3), e02204-18. https://doi.org/10.1128/AAC.02204-18

Culp, E., & Wright, G. D. (2017). Bacterial proteases, untapped antimicrobial drug targets. *The Journal of Antibiotics*, *70*(4), 366–377. https://doi.org/10.1038/ja.2016.138

Dérozier, S., Nicolas, P., Mäder, U., & Guérin, C. (2021). Genoscapist: Online exploration of quantitative profiles along genomes via interactively customized graphical representations. *Bioinformatics*, *37*(17), 2747–2749. https://doi.org/10.1093/bioinformatics/btab079

Derré, I., Rapoport, G., & Msadek, T. (1999). CtsR, a novel regulator of stress and heat shock response, controls clp and molecular chaperone gene expression in Gram-positive bacteria. *Molecular Microbiology*, *31*(1), 117–131. https://doi.org/10.1046/j.1365-2958.1999.01152.x

Dougan, D. A., Mogk, A., Zeth, K., Turgay, K., & Bukau, B. (2002). AAA+ proteins and substrate recognition, it all depends on their partner in crime. *FEBS Letters*, *529*(1), 6–10. https://doi.org/10.1016/S0014-5793(02)03179-4

Earl, A. M., Losick, R., & Kolter, R. (2008). Ecology and genomics of Bacillus subtilis. *Trends in Microbiology*, *16*(6), 269. https://doi.org/10.1016/j.tim.2008.03.004

Fimlaid, K. A., & Shen, A. (2015). Diverse Mechanisms Regulate Sporulation Sigma Factor Activity in the Firmicutes. *Current Opinion in Microbiology*, *24*, 88–95. https://doi.org/10.1016/j.mib.2015.01.006

Frandsen, N., Barák, I., Karmazyn-Campelli, C., & Stragier, P. (1999). Transient gene asymmetry during sporulation and establishment of cell specificity in Bacillus subtilis. *Genes & Development*, *13*(4), 394–399.

Fuhrmann, J., Schmidt, A., Spiess, S., Lehner, A., Turgay, K., Mechtler, K., Charpentier, E., & Clausen, T. (2009). McsB Is a Protein Arginine Kinase That Phosphorylates and Inhibits the Heat-Shock Regulator CtsR. *Science*, *324*(5932), 1323–1327. https://doi.org/10.1126/science.1170088

Gao, W., Kim, J.-Y., Anderson, J. R., Akopian, T., Hong, S., Jin, Y.-Y., Kandror, O., Kim, J.-W., Lee, I.-A., Lee, S.-Y., McAlpine, J. B., Mulugeta, S., Sunoqrot, S., Wang, Y., Yang, S.-H., Yoon, T.-M., Goldberg, A. L., Pauli, G. F., Suh, J.-W., … Cho, S. (2015). The cyclic peptide ecumicin targeting ClpC1 is active against Mycobacterium tuberculosis in vivo. *Antimicrobial Agents and Chemotherapy*, *59*(2), 880–889. https://doi.org/10.1128/AAC.04054-14

Gavrish, E., Sit, C. S., Cao, S., Kandror, O., Spoering, A., Peoples, A., Ling, L., Fetterman, A., Hughes, D., Bissell, A., Torrey, H., Akopian, T., Mueller, A., Epstein, S., Goldberg, A., Clardy, J., & Lewis, K. (2014). Lassomycin, a ribosomally synthesized cyclic peptide, kills mycobacterium tuberculosis by targeting the ATP-dependent protease ClpC1P1P2. *Chemistry & Biology*, *21*(4), 509–518. https://doi.org/10.1016/j.chembiol.2014.01.014

Gerth, U., Kirstein, J., Mostertz, J., Waldminghaus, T., Miethke, M., Kock, H., & Hecker, M. (2004). Fine-Tuning in Regulation of Clp Protein Content in Bacillus subtilis. *Journal of Bacteriology*, *186*(1), 179–191. https://doi.org/10.1128/JB.186.1.179-191.2004

Gottesman, S., & Maurizi, M. R. (1992). Regulation by proteolysis: Energy-dependent proteases and their targets. *Microbiological Reviews*, *56*(4), 592–621.

Haldenwang, W. G. (1995). The sigma factors of Bacillus subtilis. *Microbiological Reviews*, *59*(1), 1–30.

Harwood, C. R. (2007). Bacillus subtilis as a Model for Bacterial Systems Biology. In *eLS*. John Wiley & Sons, Ltd. https://doi.org/10.1002/9780470015902.a0002027

Harwood, C.R., & Cutting, S. M. (1990). Molecular biological methods for Bacillus. Chichester: Wiley.

He, G. (2010). The Temporal and Spatial Regulation of ClpP Proteases in Bacillus subtilis. Harvard University.

Ju, J., Mitchell, T., Peters, H., & Haldenwang, W. G. (1999). Sigma Factor Displacement from RNA Polymerase during Bacillus subtilis Sporulation. *Journal of Bacteriology*, *181*(16), 4969–4977.

Kain, J., He, G. G., & Losick, R. (2008). Polar Localization and Compartmentalization of ClpP Proteases during Growth and Sporulation in *Bacillus subtilis*. *Journal of Bacteriology*, *190*(20), 6749–6757. https://doi.org/10.1128/JB.00589-08

Kirstein, J., Dougan, D. A., Gerth, U., Hecker, M., & Turgay, K. (2007). The tyrosine kinase McsB is a regulated adaptor protein for ClpCP. *The EMBO Journal*, *26*(8), 2061–2070. https://doi.org/10.1038/sj.emboj.7601655

Kirstein, J., Moliere, N., Dougan, D. A., & Turgay, K. (2009). Adapting the machine: Adaptor proteins for Hsp100/Clp and AAA+ proteases. *Nature Reviews Microbiology*, *7*(8), 589.

Kirstein, J., Schlothauer, T., Dougan, D. A., Lilie, H., Tischendorf, G., Mogk, A., Bukau, B., & Turgay, K. (2006). Adaptor protein controlled oligomerization activates the AAA+ protein ClpC. *The EMBO Journal*, *25*(7), 1481–1491. https://doi.org/10.1038/sj.emboj.7601042

Kirstein, J., Strahl, H., Molière, N., Hamoen, L. W., & Turgay, K. (2008). Localization of general and regulatory proteolysis in Bacillus subtilis cells. *Molecular Microbiology*, *70*(3), 682. https://doi.org/10.1111/j.1365-2958.2008.06438.x

Kirstein, J., Zühlke, D., Gerth, U., Turgay, K., & Hecker, M. (2005). A tyrosine kinase and its activator control the activity of the CtsR heat shock repressor in B. subtilis. *The EMBO Journal*, *24*(19), 3435–3445. https://doi.org/10.1038/sj.emboj.7600780

Kleinstiver, B. P., Pattanayak, V., Prew, M. S., Tsai, S. Q., Nguyen, N. T., Zheng, Z., & Joung, J. K. (2016). High-fidelity CRISPR–Cas9 nucleases with no detectable genome-wide off-target effects. *Nature*, *529*(7587), 490–495. https://doi.org/10.1038/nature16526

Konovalova, A., Søgaard-Andersen, L., & Kroos, L. (2014). Regulated proteolysis in bacterial development. *FEMS Microbiology Reviews*, *38*(3), 493–522. https://doi.org/10.1111/1574-6976.12050

Krüger, E., & Hecker, M. (1998). The First Gene of the Bacillus subtilis clpC Operon, ctsR, Encodes a Negative Regulator of Its Own Operon and Other Class III Heat Shock Genes. *Journal of Bacteriology*, *180*(24), 6681–6688.

Krüger, E., Msadek, T., & Hecker, M. (1996). Alternate promoters direct stress-induced transcription of the Bacillus subtilis clpC operon. *Molecular Microbiology*, *20*(4), 713–723. https://doi.org/10.1111/j.1365-2958.1996.tb02511.x

Krüger, E., Völker, U., & Hecker, M. (1994). Stress induction of clpC in Bacillus subtilis and its involvement in stress tolerance. *Journal of Bacteriology*, *176*(11), 3360–3367.

Krüger, E., Witt, E., Ohlmeier, S., Hanschke, R., & Hecker, M. (2000). The Clp Proteases of Bacillus subtilisAre Directly Involved in Degradation of Misfolded Proteins. *Journal of Bacteriology*, *182*(11), 3259–3265. https://doi.org/10.1128/jb.182.11.3259-3265.2000

Kunst, F., Ogasawara, N., Moszer, I., Albertini, A. M., Alloni, G., Azevedo, V., Bertero, M. G., Bessières, P., Bolotin, A., Borchert, S., Borriss, R., Boursier, L., Brans, A., Braun, M., Brignell, S. C., Bron, S., Brouillet, S., Bruschi, C. V., Caldwell, B., … Danchin, A. (1997). The complete genome sequence of the Gram-positive bacterium Bacillus subtilis. *Nature*, *390*(6657), 249–256. https://doi.org/10.1038/36786

Labana, P., Dornan, M. H., Lafrenière, M., Czarny, T. L., Brown, E. D., Pezacki, J. P., & Boddy, C. N. (2021). Armeniaspirols inhibit the AAA+ proteases ClpXP and ClpYQ leading to cell division arrest in Gram-positive bacteria. *Cell Chemical Biology*, *28*(12), 1703-1715.e11. https://doi.org/10.1016/j.chembiol.2021.07.001

LaPelusa, A., & Kaushik, R. (2025). Physiology, Proteins. In *StatPearls*. StatPearls Publishing. http://www.ncbi.nlm.nih.gov/books/NBK555990/

Li, C., Wen, A., Shen, B., Lu, J., Huang, Y., & Chang, Y. (2011). FastCloning: A highly simplified, purification-free, sequence- and ligation-independent PCR cloning method. *BMC Biotechnology*, *11*(1), 92. https://doi.org/10.1186/1472-6750-11-92

Liu, H., & Naismith, J. H. (2008). An efficient one-step site-directed deletion, insertion, single and multiple-site plasmid mutagenesis protocol. *BMC Biotechnology*, *8*, 91. https://doi.org/10.1186/1472-6750-8-91

Mahmoud, S. A., & Chien, P. (2018). Regulated Proteolysis in Bacteria. *Annual Review of Biochemistry*, *87*, 677–696. https://doi.org/10.1146/annurev-biochem-062917-012848

Mashruwala, A. A., Eilers, B. J., Fuchs, A. L., Norambuena, J., Earle, C. A., van de Guchte, A., Tripet, B. P., Copié, V., & Boyd, J. M. (2019). The ClpCP Complex Modulates Respiratory Metabolism in Staphylococcus aureus and Is Regulated in a SrrAB-Dependent Manner. *Journal of Bacteriology*, *201*(15), e00188-19. https://doi.org/10.1128/JB.00188-19

Massoni, S. C., Evans, N. J., Hantke, I., Fenton, C., Torpey, J. H., Collins, K. M., Krysztofinska, E. M., Muench, J. H., Thapaliya, A., Martínez-Lumbreras, S., Hart Ferrell, S., Slater, C., Wang, X., Fekade, R., Obwar, S., Yin, S., Vazquez, A., Prior, C. B., Turgay, K., … Camp, A. H. (2025). MdfA is a novel ClpC adaptor protein that functions in the developing *Bacillus subtilis* spore. *Genes & Development*, *39*(7–8), 510–523. https://doi.org/10.1101/gad.352498.124

Maupin-Furlow, J. (2011). Proteasomes and protein conjugation across domains of life. *Nature Reviews. Microbiology*, *10*(2), 100–111. https://doi.org/10.1038/nrmicro2696

Maurer, M., Linder, D., Franke, K. B., Jäger, J., Taylor, G., Gloge, F., Gremer, S., Le Breton, L., Mayer, M. P., Weber-Ban, E., Carroni, M., Bukau, B., & Mogk, A. (2019). Toxic Activation of an AAA+ Protease by the Antibacterial Drug Cyclomarin A. *Cell Chemical Biology*, *26*(8), 1169-1179.e4. https://doi.org/10.1016/j.chembiol.2019.05.008

Mayangsari, R. (2018). Expression of the ClpC Protease Chaperon Gene During Sporulation in Bacillus subtilis. Mount Holyoke College.

McKenney, P. T., Driks, A., & Eichenberger, P. (2013). The Bacillus subtilis endospore: Assembly and functions of the multilayered coat. *Nature Reviews. Microbiology*, *11*(1), 33–44. https://doi.org/10.1038/nrmicro2921

Meeske, A. J., Rodrigues, C. D. A., Brady, J., Lim, H. C., Bernhardt, T. G., & Rudner, D. Z. (2016). High-Throughput Genetic Screens Identify a Large and Diverse Collection of New Sporulation Genes in Bacillus subtilis. *PLOS Biology*, *14*(1), e1002341. https://doi.org/10.1371/journal.pbio.1002341

Meisner, J., Wang, X., Serrano, M., Henriques, A. O., & Moran, C. P. (2008). A channel connecting the mother cell and forespore during bacterial endospore formation. *Proceedings of the National Academy of Sciences of the United States of America*, *105*(39), 15100–15105. https://doi.org/10.1073/pnas.0806301105

Miethke, M., Hecker, M., & Gerth, U. (2006). Involvement of Bacillus subtilis ClpE in CtsR Degradation and Protein Quality Control. *Journal of Bacteriology*, *188*(13), 4610–4619. https://doi.org/10.1128/JB.00287-06

Molière, N., & Turgay, K. (2013). General and regulatory proteolysis in Bacillus subtilis. *Sub-Cellular Biochemistry*, *66*, 73–103. https://doi.org/10.1007/978-94-007-5940-4_4

Nair, S., Milohanic, E., & Berche, P. (2000). ClpC ATPase Is Required for Cell Adhesion and Invasion of Listeria monocytogenes. *Infection and Immunity*, *68*(12), 7061–7068.

Nicolas, P., Mäder, U., Dervyn, E., Rochat, T., Leduc, A., Pigeonneau, N., Bidnenko, E., Marchadier, E., Hoebeke, M., Aymerich, S., Becher, D., Bisicchia, P., Botella, E., Delumeau, O., Doherty, G., Denham, E. L., Fogg, M. J., Fromion, V., Goelzer, A., … Noirot, P. (2012). Condition-Dependent Transcriptome Reveals High-Level Regulatory Architecture in Bacillus subtilis. *Science*, *335*(6072), 1103–1106. https://doi.org/10.1126/science.1206848

Nkomboni, S. (2017). Uncovering the Transcriptional Regulation of clpC during Sporulation in Bacillus Subtilis. Mount Holyoke College.

Pan, Q., Garsin, D. A., & Losick, R. (2001). Self-Reinforcing Activation of a Cell-Specific Transcription Factor by Proteolysis of an Anti-σ Factor in *B. subtilis*. *Molecular Cell*, *8*(4), 873–883. https://doi.org/10.1016/S1097-2765(01)00362-8

Pan, Q., & Losick, R. (2003). Unique degradation signal for ClpCP in Bacillus subtilis. *Journal of Bacteriology*, *185*(17), 5275–5278. https://doi.org/10.1128/JB.185.17.5275-5278.2003

Piggot, P. J., & Hilbert, D. W. (2004). Sporulation of *Bacillus subtilis*. *Current Opinion in Microbiology*, *7*(6), 579–586. https://doi.org/10.1016/j.mib.2004.10.001

Quigley, F. (2023). Exploring the Role of the Protein-Kinase McsB in the ClpC/MicA Protein Degradation System During Bacillus subtilis Sporulation. Mount Holyoke College.

Reder, A., Gerth, U., & Hecker, M. (2012). Integration of σB Activity into the Decision-Making Process of Sporulation Initiation in Bacillus subtilis. *Journal of Bacteriology*, *194*(5), 1065–1074. https://doi.org/10.1128/jb.06490-11

Reinhardt, L., Thomy, D., Lakemeyer, M., Westermann, L. M., Ortega, J., Sieber, S. A., Sass, P., & Brötz-Oesterhelt, H. (2022). Antibiotic Acyldepsipeptides Stimulate the Streptomyces Clp-ATPase/ClpP Complex for Accelerated Proteolysis. *mBio*, *13*(6), e01413-22. https://doi.org/10.1128/mbio.01413-22

Riley, E. P., Lyda, J. A., Reyes-Matte, O., Sugie, J., Kasu, I. R., Enustun, E., Armbruster, E. G., Ravishankar, S., Isaacson, R. L., Camp, A. H., Lopez-Garrido, J., & Pogliano, K. (2025). Developmentally regulated proteolysis by MdfA and ClpCP mediates metabolic differentiation during Bacillus subtilis sporulation. *Genes & Development*, *39*(7–8), 524–537. https://doi.org/10.1101/gad.352535.124

Rodriguez Ayala, F., Bartolini, M., & Grau, R. (2020). The Stress-Responsive Alternative Sigma Factor SigB of Bacillus subtilis and Its Relatives: An Old Friend With New Functions. *Frontiers in Microbiology*, *11*. https://doi.org/10.3389/fmicb.2020.01761

Sachla, A. J., Alfonso, A. J., & Helmann, J. D. (2021). A Simplified Method for CRISPR-Cas9 Engineering of Bacillus subtilis. *Microbiology Spectrum*, *9*(2), e00754. https://doi.org/10.1128/Spectrum.00754-21

Sauer, R. T., & Baker, T. A. (2011). AAA+ Proteases: ATP-Fueled Machines of Protein Destruction. *Annual Review of Biochemistry*, *80*(Volume 80, 2011), 587–612. https://doi.org/10.1146/annurev-biochem-060408-172623

Sauer, R. T., Bolon, D. N., Burton, B. M., Burton, R. E., Flynn, J. M., Grant, R. A., Hersch, G. L., Joshi, S. A., Kenniston, J. A., Levchenko, I., Neher, S. B., Oakes, E. S. C., Siddiqui, S. M., Wah, D. A., & Baker, T. A. (2004). Sculpting the Proteome with AAA+ Proteases and Disassembly Machines. *Cell*, *119*(1), 9–18. https://doi.org/10.1016/j.cell.2004.09.020

Schaeffer, P., Millet, J., & Aubert, J. P. (1965). Catabolic repression of bacterial sporulation. *Proceedings of the National Academy of Sciences of the United States of America*, *54*(3), 704–711.

Schlothauer, T., Mogk, A., Dougan, D. A., Bukau, B., & Turgay, K. (2003). MecA, an adaptor protein necessary for ClpC chaperone activity. *Proceedings of the National Academy of Sciences*, *100*(5), 2306–2311. https://doi.org/10.1073/pnas.0535717100

Setlow, P. (2006). Spores of Bacillus subtilis: Their resistance to and killing by radiation, heat and chemicals. *Journal of Applied Microbiology*, *101*(3), 514–525. https://doi.org/10.1111/j.1365-2672.2005.02736.x

Singh, L. K., Dhasmana, N., Sajid, A., Kumar, P., Bhaduri, A., Bharadwaj, M., Gandotra, S., Kalia, V. C., Das, T. K., Goel, A. K., Pomerantsev, A. P., Misra, R., Gerth, U., Leppla, S. H., & Singh, Y. (2015). clpC operon regulates cell architecture and sporulation in Bacillus anthracis. *Environmental Microbiology*, *17*(3), 855–865. https://doi.org/10.1111/1462-2920.12548

Su, Y., Liu, C., Fang, H., & Zhang, D. (2020). Bacillus subtilis: A universal cell factory for industry, agriculture, biomaterials and medicine. *Microbial Cell Factories*, *19*(1), 173. https://doi.org/10.1186/s12934-020-01436-8

Tan, I. S., & Ramamurthi, K. S. (2014). Spore formation in Bacillus subtilis. *Environmental Microbiology Reports*, *6*(3), 212–225. https://doi.org/10.1111/1758-2229.12130

Tevethia, M. J., Baptist, J. N., & Mandel, M. (1974). Pleiotropic Effects of Suppressor Mutations in Bacillus subtilis. *Journal of Bacteriology*, *119*(3), 961–975. https://doi.org/10.1128/jb.119.3.961-975.1974

Turgay, K., Hahn, J., Burghoorn, J., & Dubnau, D. (1998). Competence in Bacillus subtilis is controlled by regulated proteolysis of a transcription factor. *The EMBO Journal*, *17*(22), 6730–6738. https://doi.org/10.1093/emboj/17.22.6730

Wilson, G. A., & Bott, K. F. (1968). Nutritional Factors Influencing the Development of Competence in the Bacillus subtilis Transformation System. *Journal of Bacteriology*, *95*(4), 1439–1449.

Wösten, M. (1998). Eubacterial sigma-factors. *FEMS Microbiology Reviews*, *22*(3), 127–150. https://doi.org/10.1016/S0168-6445(98)00011-4

Zeigler, D. R., Prágai, Z., Rodriguez, S., Chevreux, B., Muffler, A., Albert, T., Bai, R., Wyss, M., & Perkins, J. B. (2008). The Origins of 168, W23, and Other Bacillus subtilis Legacy Strains. *Journal of Bacteriology*, *190*(21), 6983–6995. https://doi.org/10.1128/JB.00722-08

Zhu, D., Sorg, J. A., & Sun, X. (2018). Clostridioides difficile Biology: Sporulation, Germination, and Corresponding Therapies for C. difficile Infection. *Frontiers in Cellular and Infection Microbiology*, *8*. https://doi.org/10.3389/fcimb.2018.00029

APPENDIX

R script for Fluorescence Intensity Data Analysis

```
library(dplyr)
library(splines)

modified_data <- KPB1 %>%

modified_data <- BJK510 %>%
  select(`rel x...2`, int...3, `rel x...6`, int...7, `rel x...10`, int...11, `rel x...14`,
int...15, `rel x...18`, int...19, `rel x...22`, int...23, `rel x...26`, int...27, `rel x...30`,
int...31, `rel x...34`, int...35, `rel x...38`, int...39)

colnames(modified_data) <- c("x_1", "int_1",
                             "x_2", "int_2",
                             "x_3", "int_3",
                             "x_4", "int_4",
                             "x_5", "int_5",
                             "x_6", "int_6",
                             "x_7", "int_7",
                             "x_8", "int_8",
                             "x_9", "int_9",
                             "x_10", "int_10")

df <- modified_data

xCommon <- seq(0, 1, by = 0.02)
numpoints <- length(xCommon)
numberOfCurves <- 10

# Initialize a data frame to store interpolated curves
interp_df <- data.frame(rel_length = xCommon)

for (k in 1:numberOfCurves) {
  thisx <- df[[paste0("x_", k)]]
  thisy <- df[[paste0("int_", k)]]

  # Perform spline interpolation
  splineInterp <- spline(thisx, thisy, xout = xCommon)

  # Add interpolated y-values as a new column
  interp_df[[paste0("cell_", k)]] <- splineInterp$y
}
```

```
# View the interpolated data (first few rows)
head(interp_df)

library(tidyr)
# Convert wide to long format
long_data <- interp_df %>%
  pivot_longer(cols = starts_with("cell_"),
               names_to = "cell_id",
               values_to = "intensity") %>%
  arrange(cell_id, rel_length)

write.csv(long_data, "interpolated_raw_data.csv", row.names = FALSE)
```